Photochemistry of Eumelanin Precursors Role of Excited State Proton Transfer for UV Photoprotection

Corani, Alice

2015

Photochemistry of Eumelanin Precursors

Role of Excited State Proton Transfer for UV Photoprotection

Alice Corani

LUNDS UNIVERSITET

DOCTORAL DISSERTATION
by due permission of the Faculty of Science, Lund University, Sweden.

To be defended at lecture hall F, Kemicentrum, Getingevägen 60, Lund, Tuesday, 8 September 2015, 10:00

Faculty opponent

Prof. **Dan Huppert**, School of Chemistry, Tel Aviv University, Israel

Organization: **Lund University, Chemistry Department, Division of Chemical Physics, P.O. Box 124 SE-221 00, Lund, Sweden**	Document name: **Doctoral Dissertation** Date of issue: **2015-08-13**

Author(s): **Alice Corani**

Title: **Photochemistry of Eumelanin Precursors: Role of Excited State Proton Transfer for UV Photoprotection**

Abstract

Melanin is an epidermal pigment commonly known to give darker skin coloration under sun exposure. It is also present in the hair, eyes, inner ear and brain. The first function of epidermis melanin is believed to be photoprotective against harmful ultraviolet (UV) light, but the recent increase of skin cancer correlated to an increase of sun exposure questions the properties of melanin. Its presence in different body parts suggests that its function is not solely protective against UV-light.

Melanin in epidermis is divided in two categories eumelanin responsible of the dark coloration and pheomelanin, which does not have great influence on the skin shade, but gives the red coloration of hair. The amount of skin cancer has been observed to be greater in patients presenting a fair type of skin. The mechanism after melanin UV absorption is poorly understood. Two main problems arise in the study of melanin photochemistry. First the pigment is believed to be an oligomer assembly of different sizes, resulting in a broad heterogeneity of a studied sample, which makes the distinction of active species difficult. On the other hand, this is probably a key property of melanin, to ensure a photoprotective barrier against especially UV-light. The second main difficulty in the study of melanin is the solubility. The larger the pigment the less soluble in aqueous solution. An additional issue in the study of melanin is the reproducibility of the sample.

The work presented here focuses on eumelanin and its interaction with UV-light. With help of fluorescence steady state and time-resolved methods we have investigated eumelanin photochemistry. We present here a model of the energy dissipation mechanism of the pigment after UV absorption. Our method is based first on the study of synthetic samples, which allows us to have control over the heterogeneity and thus identify the function of each molecule involved in the whole melanin structure. Secondly, we have performed a bottom up approach, starting with the study of monomer constituents up to the polymer. Moreover, we have developed a method to solubilize the polymer, which does not interfere with the photodynamics of the molecules.

We demonstrate that the main dissipation channel of eumelanin after UV absorption in aqueous solution is controlled by Excited State Proton Transfer (ESPT). The surrounding solvent is essential to have a rapid and efficient UV dissipation on the order of hundreds of femtoseconds. We show that the melanin precursor DHICA, in its polymeric form, is much more efficient than the DHI precursor in the dissipation mechanism. Our approach brings new insight to the eumelanin photochemistry and shows that one of the eumelanin components has great photoprotection properties against UV-light, while the other one present longer excited state lifetimes that leave more time to the molecule to produce radicals and reactive species, possibly responsible of melanoma formation. We hope to have brought a better understanding to the property of the black polymer and opened a way to deepen the study of melanin and its interaction with UV-light.

Key words: **Melanin, Eumelanin, Photochemistry, Excited State Proton Transfer (ESPT), Fluorescence spectroscopy, Time-resolved**.

Classification system and/or index terms (if any)		Language: **English**
Supplementary bibliographical information		ISBN (print): **978-91-7623-422-8** ISBN (pdf): **978-91-7623-423-5**
ISSN and key title		Price
Recipient's notes	Number of pages:	Security classification

Signature  Date 2015-08-03

Photochemistry of Eumelanin Precursors

Role of Excited State Proton Transfer for UV Photoprotection

Alice Corani

LUNDS UNIVERSITET

Naturvetenskapliga fakulteten, Kemisk fysik
ISBN 978-91-7623-422-8

Tryckt i Sverige av Media-Tryck, Lunds universitet
Lund 2015

A mon père,

Content

Abstract

Melanin is an epidermal pigment commonly known to give darker skin coloration under sun exposure. It is also present in the hair, eyes, inner ear and brain. The first function of epidermis melanin is believed to be photoprotective against harmful ultraviolet (UV) light, but the recent increase of skin cancer correlated to an increase of sun exposure questions the properties of melanin. Its presence in different body parts suggests that its function is not solely protective against UV-light.

Melanin in epidermis is divided in two categories eumelanin responsible of the dark coloration and pheomelanin, which does not have great influence on the skin shade, but gives the red coloration of hair. The amount of skin cancer has been observed to be greater in patients presenting a fair type of skin. The mechanism after melanin UV absorption is poorly understood. Two main problems arise in the study of melanin photochemistry. First the pigment is believed to be an oligomer assembly of different sizes, resulting in a broad heterogeneity of a studied sample, which makes the distinction of active species difficult. On the other hand, this is probably a key property of melanin, to ensure a photoprotective barrier against especially UV-light. The second main difficulty in the study of melanin is the solubility. The larger the pigment the less soluble in aqueous solution. An additional issue in the study of melanin is the reproducibility of the sample.

The work presented here focuses on eumelanin and its interaction with UV-light. With help of fluorescence steady state and time-resolved methods we have investigated eumelanin photochemistry. We present here a model of the energy dissipation mechanism of the pigment after UV absorption. Our method is based first on the study of synthetic samples, which allows us to have control over the heterogeneity and thus identify the function of each molecule involved in the whole melanin structure. Secondly, we have performed a bottom up approach, starting with the study of monomer constituents up to the polymer. Moreover, we have developed a method to solubilize the polymer, which does not interfere with the photodynamics of the molecules.

We demonstrate that the main dissipation channel of eumelanin after UV absorption in aqueous solution is controlled by Excited State Proton Transfer (ESPT). The surrounding solvent is essential to have a rapid and efficient UV dissipation on the order of hundreds of femtoseconds. We show that the melanin precursor DHICA, in its polymeric form, is much more efficient than the DHI precursor in the dissipation mechanism. Our approach brings new insight to the eumelanin photochemistry and shows that one of the eumelanin components has great photoprotection properties against UV-light, while the other one present longer excited state lifetimes that leave more time to the molecule to produce radicals and reactive species, possibly responsible of melanoma formation. We hope to have brought a better understanding to the property of the black polymer and opened a way to deepen the study of melanin and its interaction with UV-light.

Populärvetenskaplig Sammanfattning

Melanin är ett pigment som finns i många olika slags vävnader. I hud och hår finns två slags melanin, pheomelanin som är typiskt för rödhåriga personer och eumelanin som finns i större mängd i mörkt hår och hud. Konstaterad korrelation mellan hudcancer och solexponering motiverar forskarna att förstå mer om melanin och dess växelverkan med UV-ljus. Man vet att rödhåriga personer med ett överskott på pheomelanin har större sannolikhet att få hudcancer och att eumelanin förmodligen har en skyddseffekt mot UV ljus. Dock är kunskapen om bakomliggande ljusinducerade fotokemiska processer dålig. Därför studerar vi melanin och dess molekylära byggstenar under UV-excitation. Melanin är en stor polymer molekyl med komplicerad fotokemi. Vi börjar därför med att studera mindre byggstenar av pigmentet, från de allra minsta monomera enheterna till oligomerer och till slut hela polymeren. Studier av monomerenheter har givit viktiga insikter om de mekanismer som styr eumelanins funktion. Arbetet på dimerer visar att redan dessa ganska små enheter har samma fotokemiska processer som hela eumelaninpigmentet. Vid absorption av UV-ljus initieras en process där en vätejon, en proton, sparkas ut från pigmentet i samma ögonblick som UV-ljuset når pigmentmolekylen. Man skulle kunna likna händelseförloppet vid att melaninet gör sig av med UV-ljusets energi genom att mycket snabbt skjuta iväg en protonprojektil. Denna projektil gör i sin tur av med energin till omgivande membranvävnad i form av värme och har därmed omvandlat farlig UV-energi till ofarlig värme. Den kemiska reaktionen går oerhört snabbt, på mindre än en tusendel av en miljarddels sekund. Vi har alltså lyckats visa att protonöverföring är den aktiva mekanismen för eumelanins funktion och att denna funktion kan härledas till enheter i pigmentet som består av två eller bara ett fåtal monomera enheter. Melaninet i hudens melanocyter består av tätt packade melaninpolymerer. För att studera melaninpigmentet i en form som liknar detta har vi också studerat tunna filmer av eumelanins byggstenar, belagda på ett kvartssubstrat. Dessa preliminära studier visar att nya processer uppstår när molekylerna är tätt packade. Framtida arbete får visa vilka dessa processer är.

Acknowledgement

I would like to first thank Prof. Villy Sundström who gave me the opportunity to work on this project and welcomed me in the department. These 5 years have been a great part of my education and I really appreciated working under his supervision and expertise. I am really grateful to him for all the knowledge I could get during this period.

I was the luckiest person to have such great collaborators to help me with the project, on both scientific and personal matters. First the group of Prof. Marco D'Ischia, providing the samples, and especially Dr. Alessandro Pezzella. I really enjoyed his visits to our lab to perform experiments. Thank you Alessandro for the discussions (scientific and other) and great knowledge/feeling in cooking (food and chemical). I also thank Dr. Dimitra Markovitsi's group, particularly Dr. Thomas Gustavsson for his kindness, his time and insight about the science. I had the great pleasure to spend time in their lab for measurements.

Of course I thank Dr. Annemarie Huijser, my first co-supervisor for bringing me into the subject and giving me the knowledge about the instrument. Finally regarding the project, I don't know how to thank Dr. Amal El Nahhas, for all the help she provided me over the PhD time. For the science, the education, the organization, the esthetics etc… I also thank her for the French discussions and for sharing the first time of being a parent.

Moreover I address special thanks to Ivan Scheblykin, as scientist but also as a neighbor, all the group leaders for the help they could provide when I needed, Arkady Yartev, Donatas Zigmantas, Tõnu Pullerits, Jens Uhlig, Per Uvdal and Ebbe Nordlander .

A special thought to Torbjörn Pascher for his availability, his help on different topics and his patience even in front of basic and dull topics/questions.

I am grateful to all the people of this department who have made this journey easier, the former and actual members, especially Carlito Ponseca which I am honored to still be a friend of, Biswanath Das for entertainment outside the lab,

Mohamed Abdellah for his constant good and enthusiastic mood, Tomas Österman for all his knowledge about the Swedish system. I also thank Erik Ekengard for all the chemistry issues I encountered and all the other members to participate in the good atmosphere of the department and the help they could provide. I apologize to all lab responsibles for all the equipment I borrowed with or without asking, but I swear I gave everything back.

Many thanks go to my officemates, Torsten and Erling for supporting my noise and talking all this time.

I do not forget Maria Leuvin for her help with the administrative matters, as well as Katarina Fredriksson and Thomas Björkman.

Finally I would like to thank my parents for supporting me along my (infinite) education, my indecision and to have made me who I am. But among all, I thank JB for his patience, to have been able to bear me all these years, and to always listen to the same complaints every year for more than a decade. Thank you for always pushing me forward and being so optimistic in all situations. I think you deserve a special merit for supporting me these last months, between the pregnancies of both a baby and a thesis. I have not been a gift every day (though it could have been worse). I also thank my daughter Marisa for being so comprehensive already at two years age and I address special thoughts to the coming Mlle P.

List of papers

I. Huijser, A.; Rode, M. F.; Corani, A.; Sobolewski, A. L.; Sundstrom, V. Photophysics of indole-2-carboxylic acid in an aqueous environment studied by fluorescence spectroscopy in combination with ab initio calculations. *Physical Chemistry Chemical Physics* **2012,** *14* (6), 2078-2086.

II. Corani, A.; Huijser, A.; Iadonisi, A.; Pezzella, A.; Sundstom, V.; d'Ischia, M. Bottom-Up Approach to Eumelanin Photoprotection: Emission Dynamics in Parallel Sets of Water-Soluble 5,6-Dihydroxyindole-Based Model Systems. *Journal of Physical Chemistry B* **2012,** *116* (44), 13151-13158.

III. Corani, A.; Pezzella, A.; Pascher, T.; Gustavsson, T.; Markovitsi, D.; Huijser, A.; d'Ischia, M.; Sundstrom, V. Excited-State Proton-Transfer Processes of DHICA Resolved: From Sub-Picoseconds to Nanoseconds. *Journal of Physical Chemistry Letters* **2013,** *4* (9), 1383-1388.

IV. Corani, A.; Huijser, A.; Gustavsson, T.; Markovitsi, D.; Malmqvist, P. A.; Pezzella, A.; d'Ischia, M.; Sundstrom, V. Superior Photoprotective Motifs and Mechanisms in Eumelanins Uncovered. *Journal of the American Chemical Society* **2014,** *136* (33), 11626-11635.

V. Corani, A.; El Nahhas, A.; Pezzella, A.; Nogueira, J.J.; González, L.; d'Ischia, M.; Sundström, V. Dissecting Eumelanin Photoprotection Mechanisms: Proton-Transfer Pathways in 5,6-Dihydroxyindole Excited State Dynamics, **2015**, *Manuscript.*

My contribution:

I. I was partly involved in the steady state measurements.

II. I was involved in the experimental part and the data analysis, as well as partly in the writing of the manuscript.

III. I did most of the experiments and contributed to the writing of the manuscript.

IV. I did most of the experimental work and partly contributed to the writing of the manuscript.

V. I planned the experiments, did all the experimental work and contributed to the writing of the manuscript.

List of Abbreviations

2D	2 Dimension
5M6HI	6-hydroxy-5-methoxyindole
APD	Avalanche photodiode
CCD	Charge coupled device
DFT	Density functional theory
DHI	5,6-dihydroxyindole
DHICA	5,6-dihydroxyindole-2-carboxylic acid
DNA	Deoxyribonucleic acid
Em	Emission
ES	Excited state
ESIPT	Excited state intramolecular proton transfer
ESPT	Excited state proton transfer
eV	Electron volt
FU	Fluorescence up-conversion
FWHM	Full width half maximum
gal	galactosyl-thio substitution
GS	Ground state
GSPT	Ground state proton transfer
HB	Hydrogen bond
HOMO	Highest occupied molecular orbital
HPPO	2-(2'-hydroxyphenyl)-5-phenyloxazole
HPTS	8- hydroxypyrene 1, 3, 6 trisulfonate
Hz	Hertz
IC	Internal conversion
ICA	indole-2-carboxylic acid
ICA-A	indole-2-carboxylic acid, anionic form
ICA-N	indole-2-carboxylic acid, neutral form
IRF	Instrumental response function
ISC	Inter system crossing
KIE	Kinetic isotope effect
LUMO	Lowest unoccupied molecular orbital

MeOH	Methanol
MCP	Micro-channel plate
PES	Potential energy surface
PM	Polymer
PMT	Photomultiplier
PN	1-propyl-2-naphthol
PT	Proton transfer
PVA	poly(vinyl alcohol)
QY	Quantum yield
SC	Streak camera
TCSPC	Time correlated single photon counting
UV	Ultraviolet

1- Introduction

Melanins, which are large heterogeneous biopolymers, are known to give the coloration of skin, hair and eyes of humans. Apart from their coloration, melanins are believed to have a photo-protective function against tissue damage that may be induced by ultraviolet (UV) and visible light. The pigments are divided into three categories, pheomelanin giving yellow to red coloration, eumelanin covering black to brown shades[1,2] and neuromelanin with dark color present in the brain and inner ear. Skin only contains pheomelanin and eumelanin, and its color is mainly due to eumelanin; pheomelanin only has a small or no impact on skin coloration.[3]

1.1- Melanin properties and production

Eumelanin and pheomelanin are synthesized by the epidermal melanocytes in melanosomes as shown in Figure 1−1. Melanocytes synthesize both melanin types, according to the available hormones and precursors present in the cell. Both melanins are derived from the oxidation of dopaquinone. Eumelanin is made of indolic units and is the result of tyrosine oxidation. Pheomelanin is the product of cysteinyldopa oxidation giving benzothioazine units.[3,4] Figure 1−2 presents the biosynthetic pathways of melanin production, as well as the chemical structure of the main monomer constituents of pheomelanin and eumelanin. Eumelanin and pheomelanin structures are presented in Figure 1−3.

The activation of melanin production is not yet well understood but it is believed that the number of melanocytes increases as a response to UV radiation, which increases melanosome formation, melanin production and melanosome transfer through the epidermis.[5]

The reaction rate of melanin polymerization has been measured and the kinetics of formation of intermediates seems to preferably lead to 5,6-dihydroxyindole-2-carboxylic acid (DHICA) production, thus to eumelanin.[6] Pheomelanin synthesis requires the presence of the amino acid cysteine. It is believed that pheomelanin

production occurs when the enzyme tyrosinase, producing eumelanin, is not accessible and its activity is slow making pheomelanin the default polymerization path.[3]

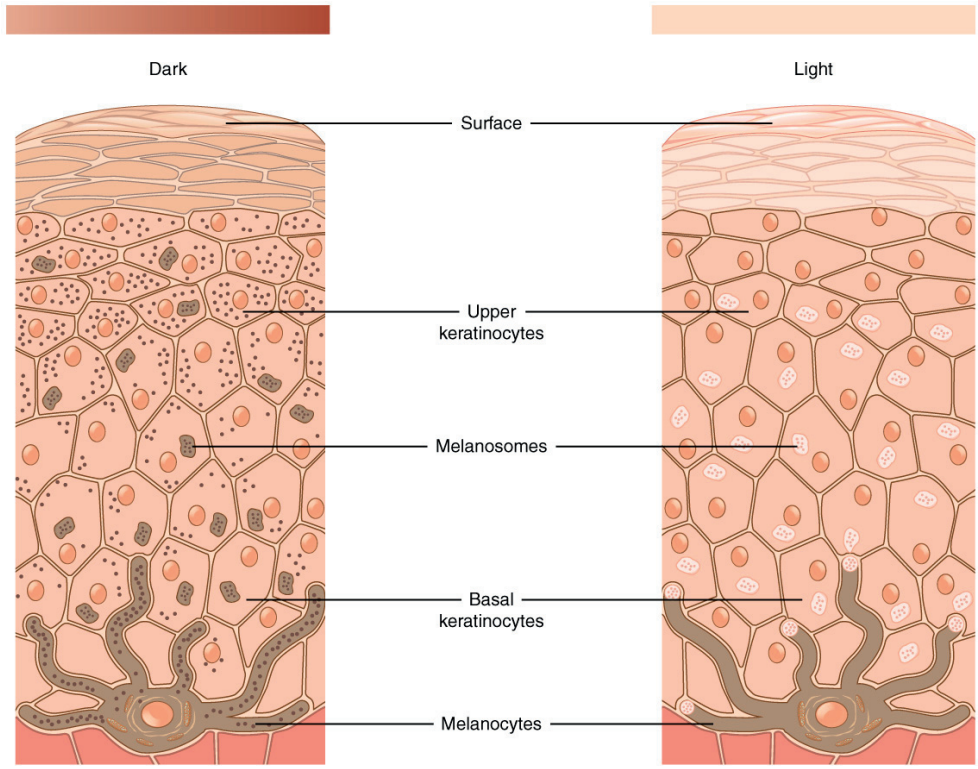

Figure 1-1: Melnocyte location and melanosome distribution containing melanin in the epidermis according to the skin coloration. Picture from http://philschatz.com/anatomy-book/resources/504_Melanocytes.jpg.

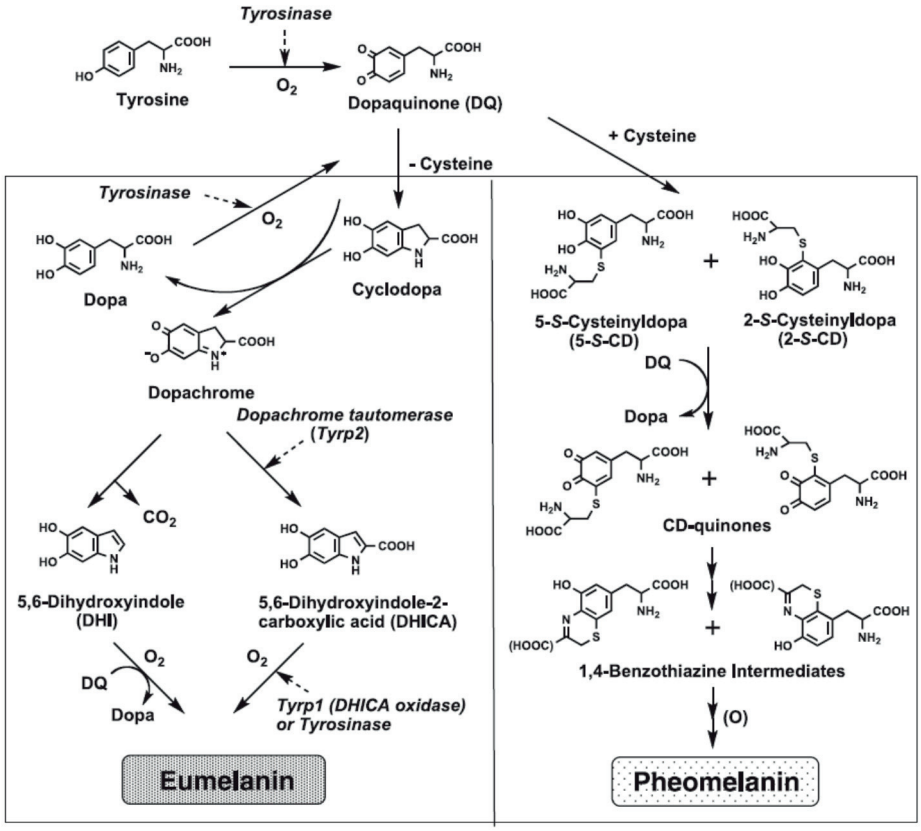

Figure 1-2: Biosynthetic pathways leading to eumelanin and pheomelanin production. Figure from Ito and Wakamatsu, 2008.[6]

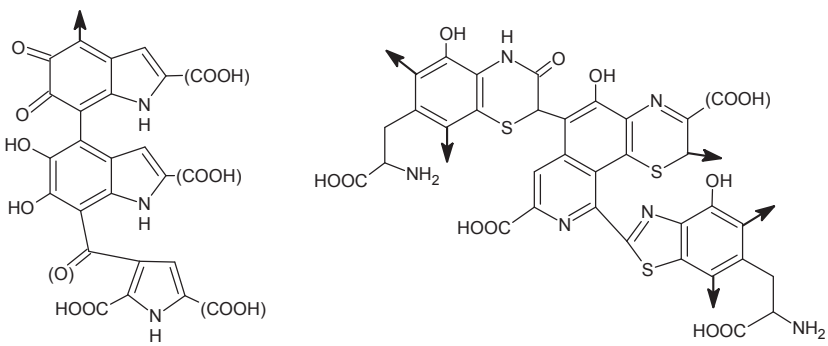

Figure 1-3: Suggested final structure of melanin polymers. Figures from ref. 6.

The large heterogeneity of melanins is an admitted fact, though their real structure is not known. Both pheomelanin and eumelanin in different proportions form the melanin pigment present in tissue. Because of its peculiar absorption spectrum[7] (Figure1−4), a monotonically decreasing absorbance with increasing wavelength, melanin was believed for years to have mainly, if not solely, a photoprotective function against UV light since the absorption in this wavelength region is highest. However, the recent increase of skin cancers, partly attributed to melanin and its precursors, has motivated researchers to obtain a better understanding of melanin photophysics and photochemistry. The presence of melanin in the brain as neuromelanin, believed to be a mix of pheo- and eumelanin monomers, suggests other melanin functions.

Latter on eumelanin is found to have photo-protective and anti-oxidant properties.[8-12] The anti-oxidant function comes from the ability of eumelanin to chelate metal ions. For instance, it has been observed that patients suffering from Parkinson's diseases have a higher proportion of free iron in the substantia nigra compared to a healthy patient. It was demonstrated that melanin forms a stable complex with iron involving the hydroxyl groups of the melanin constituents.[13-16] Iron is released by the unhealthy neuromelanin, which undergoes a redox reaction leading to cytotoxic damage of DNA and proteins.[14] Moreover, metal ions have a great influence on the dimerization of melanin monomers. Thus, it has been experimentally observed that the presence of copper ions, Cu^{2+}, stimulates dimerization at various binding sites. While 5,6-dihydroxyindole (DHI) preferably oxidizes to the 2,4' and 2,7' dimers, the presence of Cu^{2+} favores binding at the 2-positions to form the 2,2' dimer. In the case of DHICA, the presence of Cu^{2+} increases the reactivity at position 3 to produce 3,4' and 3,7' dimers, whereas in the absence of Cu^{2+} only 4,4' and 4,7' dimers are formed (see Figure 1−5 for nomenclature).[17,18]

Pheomelanin is known to be more phototoxic than eumelanin due to the higher proportion of melanoma among fair skin persons; in addition, as mentioned above, synthesis pathways of melanins seem to preferentially go toward eumelanin production.[3,8,19]

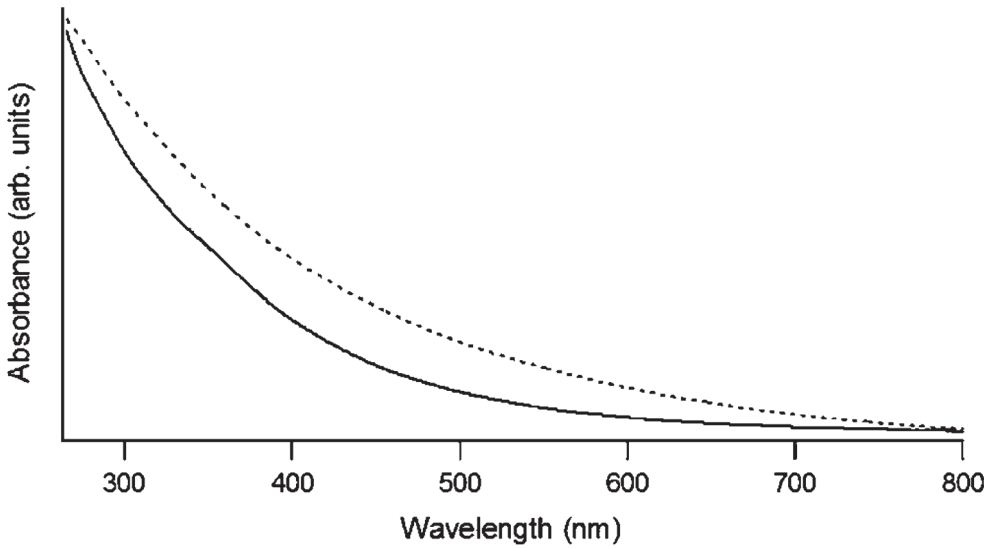

Figure 1-4: Absorption spectra of pheomelanin (solid line) and eumelanin (dashed line). Figure from Tran et al, 2006.[7]

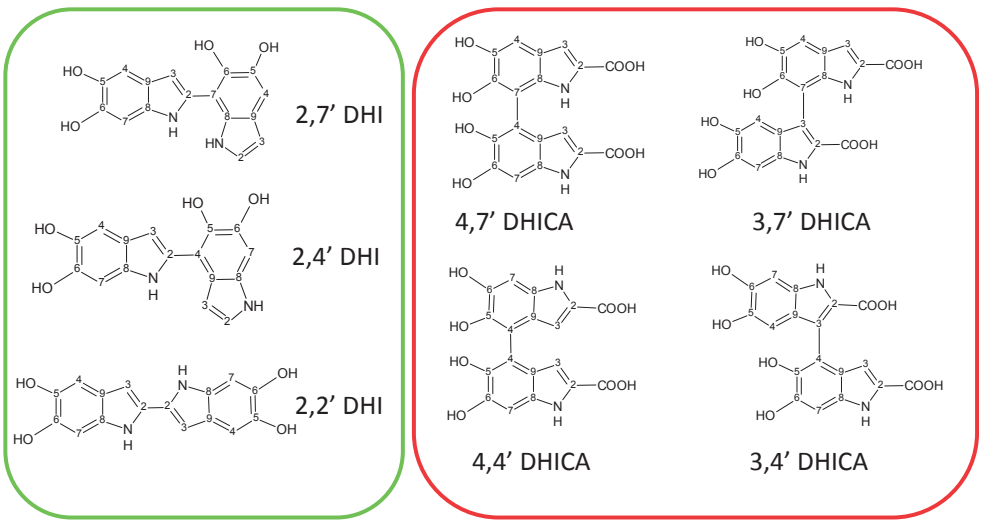

Figure 1-5: DHI and DHICA dimer structures.

The peculiar absorption spectrum of melanin has been explained as a consequence of chemical disorder[20,21] and superposition of the absorption bands of different oligomer sizes, as well as presence of different oxidation states. The structure of melanin polymers has been discussed for many years, and it is now suggested that melanin is an aggregate of closely stacked small oligomers from 4 to 8 monomer

units. From DHI/DHICA monomers and their oxidized forms a large variety of dimers can be produced, for DHI 16 different dimers can be obtained.[20] Density Functional Theory (DFT) calculations have shown that the Highest occupied molecular orbital (HOMO) – Lowest unoccupied molecular orbital (LUMO) gaps for different species, oxidized or reduced forms and tautomers, cover a large range of energies.[22-24] We can imagine that already with a limited number of species the absorption spectrum will cover a broad energy range. The oxidized monomers are known to be unstable but it has been demonstrated that oligomerization stabilizes the oxidized species.[25] A theoretical model for indolic homopolymers has shown that with only small oligomers of 5 to 6 units the absorption spectrum of melanin can be explained as a result of excited state delocalization. Moreover, recent calculations show that close stacking of small oligomers of 5 to 6 units may produce exciton delocalization, which can induce a large broadening of the absorption bands of each species. All these results are in favor of a tight stacking configuration of small oligomer units forming the melanin pigment and giving rise to the typical absorption spectrum of melanin. In addition, mass spectrometry analysis have not been able to detect large oligomers; several experiments have shown that oligomers between 4 and 8 monomer units are the main constituent of the melanin pigment.[26-31] Recently, a model based on oligomers of up to 4 monomer units could describe mass spectrometry data from melanin of several million years old fossil fish eyes, dating from the early Eocene period.[32]

Though most analysis support the stacking model, these results should be treated with care because it has been shown that sample preparation of melanin can affect the chemical structure of the melanin.[21] Light scattering has been believed to be a reason to the peculiar absorption spectrum, but measurements with highly diluted samples show that the observed absorption with gradually decreasing absorbance at visible wavelength is still present. Light scattering for highly aggregated samples is of course present and it is believed to be one of the melanin properties to efficiently protect the skin against harmful UV-radiation. However, it is commonly accepted that a small part of the measured absorption is due to scattering, but no more than 5 %.

1.2- Photochemistry of melanin

Melanin has been studied for more than 40 years, but its photochemistry still remains unclear. From its absorption spectrum it is clear that the pigment absorbs a great part of the sunlight, especially in the most energetic UV-region. However, the processes how melanin protects the skin and dissipates the absorbed energy is still poorly understood.

It has long been said that melanin does not fluoresce, but it was shown that radiative dissipation channels of the absorbed energy represent about 0.1 % for eumelanin and 0.2 % for pheomelanin.[33,34] Eumelanin has a smooth fluorescence yield spectrum, while pheomelanin exhibits a more structured spectrum. These differences might be a reason to the distinct photo-properties − the spectrally smoother energy dissipation of eumelanin could explain why eumelanin seems to be more photoprotective. Nighswander-Rempel[35] suggested that the similarities between the two polymers are due to the great chemical disorder and the differences could be explained by the way the polymers are structured (length, binding etc…). The Meredith group[33-37] managed to construct a map of the radiative quantum yield of the melanins as a function of excitation and emission wavelengths. They demonstrated that eu- and pheomelanin have different signal amplitudes, but both exhibit a higher radiative quantum yield in the UV region of the spectrum.

The overall energy dissipation process of melanin is complex − in addition to the excitation energy dependence of the response it has been demonstrated to also depend on the pigment size. This makes comparison between different studies difficult. The fluorescence decays of melanins is multipexponential.[21,38-41] Eumelanin emission at 520 nm after 320 nm excitation has been fitted using four exponential lifetimes ranging from 58 ps to 7 ns, but no information on a timescale shorter than 10 ps was provided. Synthetic pheomelanin pigment (no pure pheomelanin polymer exists in nature) shows the same general emission behavior, a nonexponential decay, but pheomelanin 520 nm emission could be fitted using only three lifetimes in the range from 50 ps to 7 ns.[38]

Transient absorption measurements on both pigments show that excitation of the polymers results in instantaneous appearance of transient absorption spectra displaying several bands. The transient spectrum decays in a few picoseconds to a time independent non-zero value. This demonstrates the formation of a long lived photoproduct. No total ground state recovery could be reached on a nanosecond

timescale.[41] The decays of the transient absorption spectra of the red and the black melanins are globally identical, and Simon et al. suggest that this similar dynamics, despite some spectral differences, is due to the similar catechol chromophore forming the polymer and that it is the main actor in the energy dissipation process of the pigment.

Photoacoustic calorimetric experiments have shown that more than 90 % of the absorbed photon energy when excited at 527 and 400 nm is dissipated as heat while only 70 % is converted to heat when 264 nm excitation is used.[42] This observation is in agreement with the higher radiative quantum yield (QY) found in the UV region, and it is explained by the presence of monomeric species, which have a much higher fluorescence QY than the oligomers. Comparison between transient absorption, photoacoustic and emission data have shown that the main relaxation channel is the non-radiative one, and after 20 ps 90 % of the excited pigments have relaxed back to the ground state.[43] The non-exponential fluorescence decays are indicative of a heterogeneous pigment composition with different components having different excited state dynamics and perhaps different relaxation mechanisms.

The complicated photochemistry of the polymeric pigment and calculations showing that a limited number of monomers can explain the optical properties of melanin, encouraged us to adopt a bottom up approach starting with the study of monomers and going up step by step to the polymer. The thesis describes work on monomers, oligomers and polymers of DHI and DHICA, with the aim to resolve excited state relaxation mechanisms and suggest mechanisms and active species for the excited state dissipation of eumelanin pigments. The results show that excited state proton transfer is a key process controlling the photochemistry and excited state dynamics of these molecules. Depending on solvent, pH and aggregation state of the monomers the timescale of proton transfer varies from sub-ps to nanoseconds. In solution, eumelanin building blocks based on DHI and DHICA have very different relaxation properties and from this work it is concluded that DHICA is critical for providing the very efficient excited state energy dissipation of eumelanin. Already a dimer of DHICA has an excited state relaxation pattern very similar to that of polymeric DHICA. Oligomeric and polymeric DHI in solution, on the other hand, have generally longer excited state lifetimes in the order of ns.

We also studied the excited state dynamics of solid thin films of DHI and DHICA monomers and polymers, as a first step towards a model system for eumelanin in

melanosomes. The experiments show that both DHI and DHICA, in both monomeric and polymeric form, exhibit very short lived excited state decays, on the picosecond or shorter timescale. This is quite different from the situation in solution phase and suggests that additional interactions are present in the solid state where melanin chromophores are densely packed. We believe that our results provide important insights into the photochemistry and photoprotective properties of eumelanin and shed light on the different roles played by DHI and DHICA in UV-energy dissipation.

2- Experimental methods

2.1- Samples

Methanol (MeOH), Sodium phosphate buffer and indole-2-carboxylic acid (ICA) molecule were purchased from Sigma Aldrich with spectroscopic grade when available.

Deuterated buffer was prepared by evaporation of sodium phosphate buffer solution of the desired pH solution and addition of the corresponding volume of D_2O (with 98 to 99 % purity).

DHICA, DHI monomer, oligomers and their derivatives were prepared by our collaborator Dr. Alessandro Pezzella from the organic chemistry group in Naples, Italy. Herein we include a brief description of the studied samples. For complete synthesis procedure the reader is kindly asked to refer to the corresponding paper.

The main samples studied for DHI were the monomer and three dimers, 2,2' 2,4' and 2,7' as well as the polymer.

DHICA studies included the monomer, two dimers the 4,4' and the 4,7', the 4,4′:7′,4″ trimer and the polymer.

Several derivatives have been studied such as the 6-hydroxy-5-methoxyindole (5M6HI), the N-methylated DHI (N-MeDHI).

Paper IV included a serie of DHIs were galactosyl-thio substitution have been performed for synthesis of the used samples described in references 44,45.

2.1.1- Monomers

Briefly, DHICA and DHI synthesis was obtained by biomimetic oxidation from L-dopa as described in 44, 5M6HI was obtained by decarboxylating the corresponding carboxylic acids in decalin2 according to ref. 46; N-MeDHI was prepared by oxidative cyclization of nor-adrenaline.[47]

The purity of all samples was over 90 % and was measured by proton NMR analysis.

2.1.2- Oligomers and Homopolymers

The 4,4' DHICA dimer was obtained from a solution of DHICA in TRIS buffer at pH 8.0 and addition of a solution of $CuSO_4$. Precipitation of the 4,4' dimer was obtained after reduction with an excess of sodium borohydride and then by acidification of the filtered solution purity.[44,48]

The other DHICA dimer, 4,7' and 4,4′:7′,4″ trimer are obtained by tyrosinase oxidation of DHICA monomer in buffer solution. They are then separated from the reaction mixture first by chemical treatment and then by chromatography. The procedure is described in ref. 48.

DHI dimers (and their acetyl derivatives) are prepared following the procedure in ref. 49. Synthesis is not straightforward and involves successive coupling, cyclization steps and protected o-ethynylaniline intermediates.

Homopolymers in solution were obtained by tyrosinase oxidation of the corresponding monomer in poly(vinyl alcohol) (PVA) /buffer solution during ~4h:

A solution of DHI or DHICA (10 mg, in 2 ml) in phosphate buffer pH 7.0 was adjusted to pH 8 by equilibration with concentrated ammonia solution. Air was bubbled through the stirred solution up to 4 hours. Before measurements glacial acetic acid was then used to adjust the pH to 7.

2.1.3- Film preparation

2.1.3.1- Monomers film

DHI and DHICA thin films were prepared by spin coating; thin films were deposited on quartz substrates. They were obtained from a 30 mg/ml solutions of DHI or DHICA in methanol after filtering through a 0.2 μm nylon membrane, using the following speed gradients: 2000 rpm for 90"; 800 rpm for 10" and 3000 rpm for 60"; 2000 rpm for 60"; and 3000 rpm for 90".

2.1.3.2- Homopolymers film

The oxidation of DHI or DHICA thin films (100-200 nm thickness) to give the melanin polymer has been achieved by exposure to an oxidizing atmosphere (e.g.

oxygen atmosphere and ammonia vapors). In the general procedure, the appropriate film was incubated in the oxygen/ammonia atmosphere at controlled temperature (25 - 40 °C). The ammonia vapors were produced by equilibration of the atmosphere with ammonia solution (28 % to 7 % NH_3 in H_2O) in a sealed chamber at 1 atm pressure. Exposure times varied in the range of 2 to 18 h. When appropriate the whole spin coating procedure was conducted under oxidation promoting atmosphere.

2.2- Fluorescence spectroscopy

The choice of fluorescence spectroscopy to probe the photoinduced mechanism of melanins seems peculiar since previous studies have demonstrated that melanins have small fluorescence quantum yields.[21,33,35,36,50] The bottom up approach we performed to get a picture of melanin photodynamics consists in studying building blocks made of rather small aromatics molecules, i.e. indole derivatives. Such conjugated systems are known to have a fair emission signal. Thus, despite the low quantum yield of both melanins and their building blocks, it turned out that fluorescence is the most convenient technique to investigate these spectroscopically complicated systems as it probes signal from the first excited state and does not contain contributions from higher excited states, or from non-emissive intermediates. Moreover, the relatively fast acquisition time of fluorescence spectra makes this technique suitable for the samples studied here, which degrade rapidly in solution and under irradiation. This is especially true for streak camera and Time Correlated Single Photon Counting (TCSPC) measurements.

2.2.1- Fluorescence principle

The emission of light after electronic excitation by photon absorption of a molecule is referred as photoluminescence. Photoluminescence is divided into two categories, fluorescence and phosphorescence.

A schematic representation of the energy absorption and dissipation of a molecule is given by the Joblonski diagram, Figure 2−1. Three states are important to describe the photochemistry of a molecule, the ground state S_0, the first excited state S_1 and the triplet state T_1. An excited molecule M is usually represented as

M*. Higher singlet or triplet excited state can also be displayed, however direct excitation to the S_2, S_3… is usually followed by rapid internal conversion (IC) to S_1 or intersystem crossing (ISC) to the T_1 state. Fluorescence decay mainly represents the relaxation from the S_1 state.

In such a diagram (Figure 2−1), it is assumed that the nuclear geometry of the ground state molecule and the excited one is similar and represents the minimum energy. The difference between the ground and the excited state molecules lies in their electronic configuration and, or spin. As shown in the Joblonski diagram the spins of S_0 and S_1 occupy different orbitals (HOMO, LUMO) and both spins are antiparallel (↑↓) in S_0 and S_1. For the triplet state, in addition to different molecular orbital occupancy the spins are parallel (↑↑).

The term singlet and triplet refer to the multiplicity of the state according to the formula:

$$\boldsymbol{M = 2S + 1} \qquad (2.1)$$

With $S = \sum s_i \; with \; s_i = +\frac{1}{2} \; or \; -\frac{1}{2}$

For an electron pair, M is equal to 3 when the spins are of the same sign (have the same direction) and 1 when they are of opposite sign (anti-parallel).

The photophysical process following photon absorption and promoting the system to a singlet excited state can be either radiative or non-radiative. Before describing the electronic radiative and non-radiative process, it is worth noting that electronic excitation is also accompanied by vibrational excitation. The excited system generally reaches a higher vibrational state and one of the first steps is then vibrational relaxation to the lowest vibrational level of the excited electronic state. This is represented by dotted arrow in Figure 2−1. Vibrational relaxation is the main reason to the observed energy difference between the absorption and fluorescence spectra, the so called Stokes shift. Other parameters influencing the Stokes shift are solvent relaxation, excited state reactions, etc. Vibrational relaxation is a non-radiative process.

The radiative processes are:

- Fluorescence, relaxation from S_1 to S_0 accompanied by the emission of a photon
- Phosphorescence, relaxation from T_1 to S_0 with photon emission

Transition from a singlet to a triplet state is forbidden due to the need of spin change, and as a consequence, phosphorescence lifetimes are usually much longer

than fluorescence ones, typically on the order of milliseconds for phosphorescence and nanoseconds for fluorescence.

The non-radiative processes are:

- Internal conversion (IC) either from a S_n state to S_{n-1}, or T_n to T_{n-1} ($n \geq 2$); IC is associated with heat dissipation.
- Intersystem crossing (ISC) from S_n to T_n ($n \geq 1$), or T_1 to S_0; the energy is also released as heat.

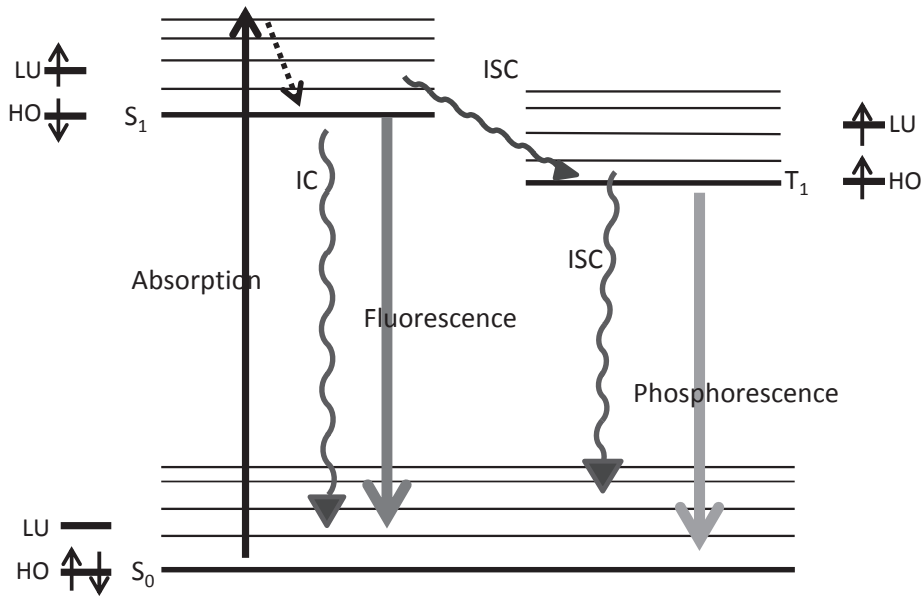

Figure 2-1: Jablonski Diagram, solid lines are processes related to absorption and emission of photons. ISC stands for Intersystem Crossing and IC for Internal Conversion. The dotted line represents vibrational relaxation from a high vibrational state to a lower one.

The Joblonski diagram is a good tool to describe the photophysics of a system but it becomes complicated for photochemical processes, where a change in the nuclear geometry happens. For such processes, potential energy surfaces (PES) better illustrate the process; ground and excited states are represented by curves where the minima of the curves along some coordinates illustrate the equilibrium geometry. Figure 2−2 illustrates a PES diagram for the Excited State Intramolecular Proton Transfer (ESIPT) process of DHICA. Excitation at specific wavelength prepares DHICA in the excited state (ES). The ES of the zwitterion

species lies at lower energy than the bottom energy of the excited DHICA. According to this diagram fast ESIPT is expected. This diagram illustrates zwitterion formation of DHICA in acidic solution that we encounter in the study of the eumelanin precursor.

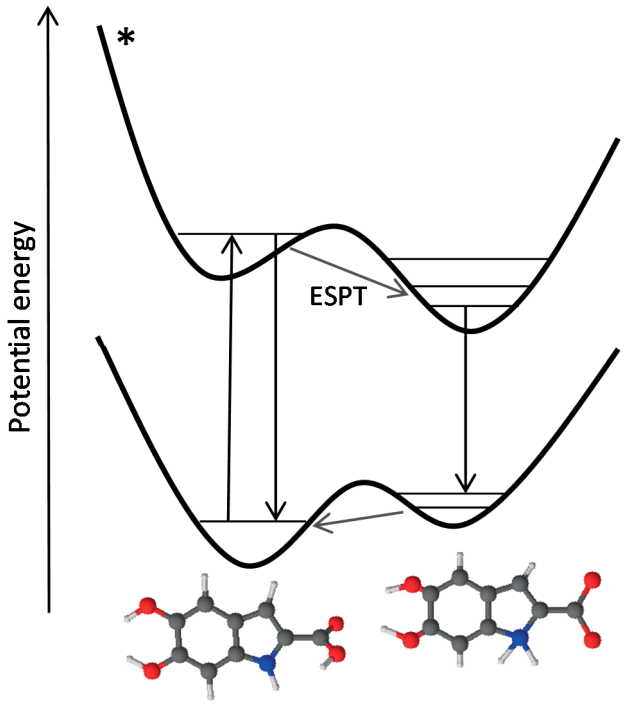

Figure 2-2: Potential energy surface describing ESIPT through a small energy barrier.

To understand the relaxation process, perhaps the most important parameters are the fluorescence lifetime and QY.

The fluorescence QY,Φ of a sytem is defined as follows,

$$\Phi = \frac{Number\ of\ emited\ photons}{Number\ of\ absorbed\ photons} \tag{2.2}$$

Or,

$$\Phi = \frac{k_r}{k_r + k_{nr}} \tag{2.3}$$

Where k_r is the radiative rate constant and k_{nr} is the total rate constant of all non-radiative processes originating from the S_1 state.

The excited state lifetime τ is defined by

$$\tau = \frac{1}{k_r + k_{nr}} = \frac{1}{k} \tag{2.4}$$

Where k is the total rate constant.

Fluorescence is a first order process and its time dependence can therefore be described by an exponential decay,

$$I_t = I_0 e^{-t/\tau} \tag{2.5}$$

where I_t is the fluorescence intensity at time t and I_0 is the initial one.

In our work, the measured fluorescence decays generally represent more than one process and therefore multiple exponential decays were used to fit the data,

$$I_t = \sum_i a_i e^{-t/\tau_i} \tag{2.6}$$

2.2.2- Time-resolved Fluorescence techniques

In order to probe the fluorescence emission as a function of time we have used three different techniques adapted to the required time resolution – time correlated single photon counting (TCSPC), fluorescence streak camera (SC) and fluorescence up-conversion (FU). All time-resolved emission measurements present the same general schematic as shown in Figure 2−3. Typically, a ~100 fs laser pulse with high repetition rate is used to excite the sample and it is focused either in reflection or transmission mode into the sample. The emission from the sample is collimated and then focused to a detector.

Our samples have their main absorption band and part of their emission in the UV part of the spectrum. Excitation was performed between 267 and 280 nm. Consequently quartz optics were used to allow UV transmission.

Both TCSPC and SC measurements used the same excitation source, 267-280 nm sub-ps pulses generated by frequency tripling 150 fs Ti:Sa laser (Spectra Physics, Tsunami) pulses (800-840 nm) in a Photop Technologies, TP-2000B, tripler. The Ti:Sa laser operated at 80 MHz repetition rate was pumped by a solid state green laser (Spectra Physics, Millenia). A small fraction of the Ti:Sa oscillator output beam was used to generate the start pulse for the TCSPC or the trigger signal for the streak camera. As depicted in Figure 2−3 the excitation light was focused onto the sample and the emission was collected through a set of collimating lenses and a polariser set at the magic angle 54.7 ° and finally focused onto the detector.

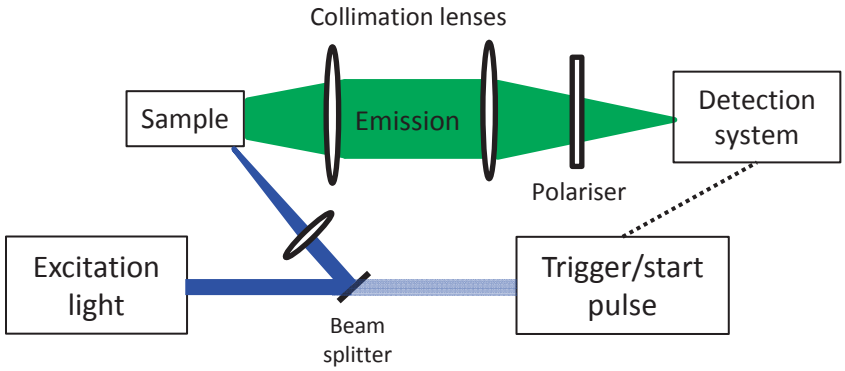

Figure 2-3: General time-resolved fluorescence measurement set up.

2.2.2.1- Time Correlated Single Photon Counting (TCSPC)

TCSPC is a highly sensitive technique, which has the advantage of using low intensity excitation and can measure very weak emission signals. However, the temporal resolution is quite limited depending mainly on the detector and the electronics. A resolution of tens of picoseconds has been obtained using a micro-channel plate (MCP) detector but the general resolution is approaching 100 ps.

TCSPC is a statistical method. Its high sensitivity lies in the fact that maximum one photon is detected per excitation pulse. A photodiode detects the excitation pulse which triggers the so called start signal. The excited sample emits a photon which is detected at a certain time after the start pulse. This information is stored in channels corresponding to a definite time range (the number of channels will determine the time increment) to build up a histogram of the detected photons. The principle is illustrated in Figure 2−4. In order to obtain the time information, a ramp voltage is started as the start pulse is detected. The photon is detected at a certain voltage corresponding to the difference between the detected photon and the start pulse.

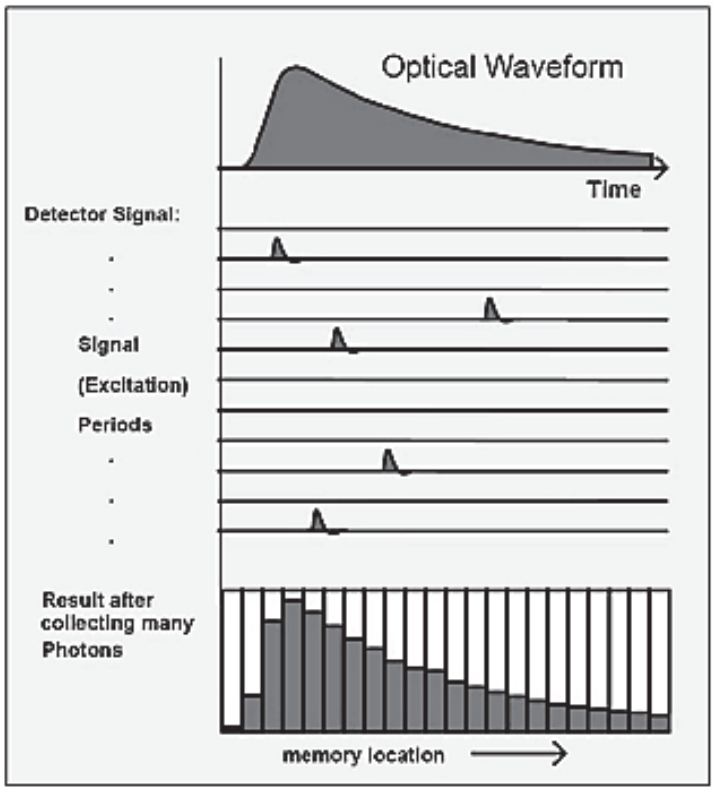

Figure 2-4: TCSPC principle - Figure from: http://smos.sogang.ac.kr/mediawiki/index.php/Time_Correlated_Single_Photon_Counting (2015-07-28).

If more than one photon is detected per excitation pulses, a pile-up effect is observed and the emission decay becomes distorted.

The limiting factors of the temporal resolution is given by the speed of the detector to detect a photon, i.e. the time it takes to convert a photon to an electrical signal. The Instrumental Response Function (IRF) is also broadened by other factors, such as the excitation pulse, the jitter given by the electronic components and the temporal resolution of the channels.

We used band pass filters (10 nm width) from 350 to 550 nm with a 50 nm increment to select the emission spectral region of interest. The emission was detected by an Avalanche PhotoDiode (APD) detector (Micro Photon Devices) and coupled to a PicoHarp 300 from Picoquant for the registration of the pulse histogram. The FWHM obtained for the IRF was about 350 ps.

2.2.2.2- Streak camera (SC)

The streak camera has the advantage over many other fluorescence techniques to provide temporal and spectral information simultaneously, which makes the data acquisition relatively fast. A 2D image can be obtained in one excitation pulse for samples with high fluorescence quantum yield. In most measurements, however, a fluorescence image is collected by averaging over millions of excitation pulses, in order to obtain good signal-to-noise. The temporal resolution obtained can reach ~2 ps.

After excitation of the sample the emitted photons are collimated via a set of quartz lenses and then focused on the slit of a spectrograph. The photons then hit a photocathode, where they are converted into photoelectrons. The photoelectrons are first accelerated and then deflected onto a phosphorous screen by sweeping a voltage between two electrodes. Before reaching the phosphorous screen they are amplified by a MCP. The electrons are finally reconverted into photons and the 2D image is recorded by a CCD camera. The principle of the streak camera is illustrated in Figure 2−5.

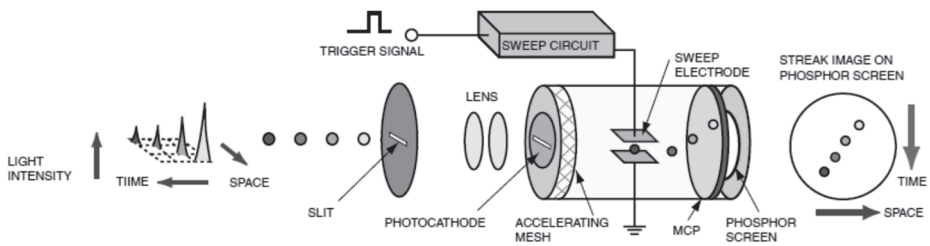

Figure 2-5: Streak tube principle, Figure from Hamamatsu, 'guide to streak camera'.

The limitation of the time resolution is mainly caused by the trigger jitter which can be quite large and makes averaging complicated for short lifetime measurement.

The streak camera Hamamatsu C6860 was used for our experiments.

2.2.2.3- Fluorescence Up-conversion (FU)

The fluorescence up-conversion system, illustrated in Figure 2-6, has the best temporal resolution among the systems mentioned above, on the order of 100 fs.

The only limitation on the time resolution is given by the excitation pulse and the thickness of the non-linear crystal used.

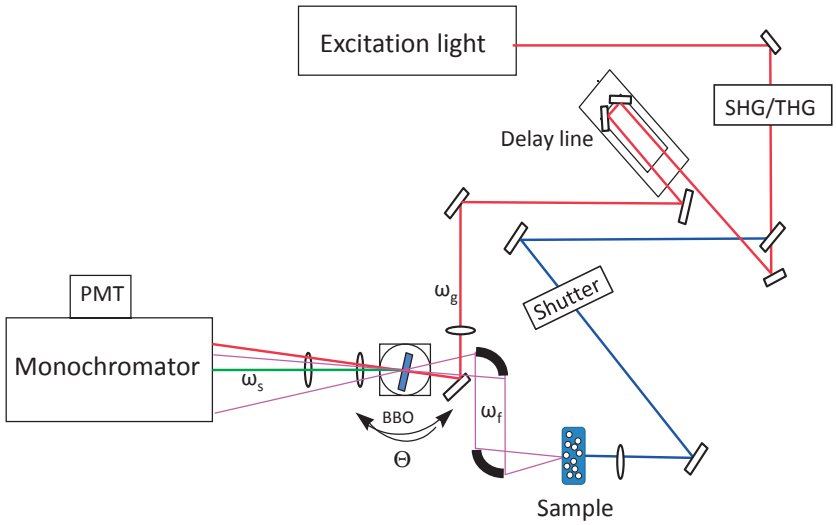

Figure 2-6: Typical fluorescence up conversion set up. SHG/THG, stand for second or third harmonic generation. PMT for photomultiplier detector.

The basic principle of the up-conversion technique is to frequency-mix the fluorescence emission from the sample and a fundamental gate pulse in a non-linear crystal. After mixing, the resulting signal frequency (ω_s) is the sum of the frequencies of the gate pulse (ω_g) and the fluorescence (ω_f) that satisfies the phase matching conditions.

$$\omega_s = \omega_g + \omega_f \qquad (2.7)$$

The up-converted signal amplitude is proportional to the fluorescence intensity. 800 nm pulses from a mode-locked Ti-Sa laser (MIRA, Coherent) was used to generate the 3rd harmonic 267 nm excitation pulse. The fluorescence was collected with parabolic mirrors and mixed with the gating pulse in a type I BBO crystal. The gate pulse is sent through an optical delay line and by varying the time-delay between the fluorescence excitation pulse and the gate pulse, the fluorecence intensity as a function of time can be obtained. The detection system consists of a monochromator to select the wavelength and a photomultiplier, which allows photon counting. The phase matching angle of the up conversion crystal is

adjusted as a function of the fluorescence wavelength. Both parallel ($I_{\parallel}$) and perpendicularly ($I_{\perp}$) polarized emission signals were measured and the emission at the magic angle (I_{MA}) was calcultated according to the following equation,

$$I_{MA} = I_{\parallel} + 2I_{\perp} \quad (2.8)$$

Details about the set up used for the experiment are described in reference 51.

The three time-resolved fluorescence techniques used in this work allowed us to record emission decays from the fs timescale up to the nanosecond one. Full spectral information was obtained with streak camera detection, while up-conversion and TCSPC provided supplementary information at selected wavelengths on different timescale.

The fluorescence techniques used for the study of melanins appeared to be efficient and appropriate methods to obtain information about excited state dynamics and photochemistry of these molecules.

3- Excited State Proton Transfer

Proton transfer (PT) has been defined as "the most common reaction in chemistry".[52] It is a frequent phenomenon in chemistry and particularly in biological systems.

In the ground state (GS), PT is defined as an acid base reaction; according to the pH of the solution and the dissociation constant K_a the concentration of the protonated and deprotonated species can be defined as follows:

For an acid AH with dissociation constant K_a:

$$AH \leftrightarrow A^- + H^+ \tag{3.1}$$

$$pH = -\log[H^+] \tag{3.2}$$

$$K_a = \frac{[A^-][H^+]}{[AH]} \tag{3.3}$$

$$pK_a = -logK_a \tag{3.4}$$

$$pH = pK_a + log\frac{[A^-]}{[AH]} \tag{3.5}$$

In the case of a negative pK_a, the majority of the species will be in the ionic form in solution; for example HCl being a strong acid ($pK_a<0$) is present in solution in the form of H_3O^+ and Cl^-. For a weak acid, when the pK_a has a positive value the concentration of the anionic species will be dependent on the pH of the solution as shown in equation (3.5).

Ground state proton transfer (GSPT) is often characterized by a large activation energy barrier and can therefore be a really slow process.

When a molecule is excited to an electronically excited state (ES), some are much stronger acids (also true for some bases) than in the ground state. These molecules

are called photoacids, and their pK_a in the excited state, pK_a^*, can be characterized by a decrease of several pH units as compared to their GS pK_a.

Photoacid molecules are typically aromatic molecules possessing an alcohol group like phenol, but excited state proton transfer (ESPT) has also been observed for aromatic amines like 7-Azaindole.[53-56] ESPT can be divided in two categories: 1) when a molecule possesses a proton donor and a proton acceptor group, the PT happens within the molecule, the process is referred as Excited State Intramolecular Proton Transfer (ESIPT) and the obtained photoproduct is a tautomer. 2) When the acceptor group is either another molecule or the surrounding solvent acting as a base, the process is referred to Excited State Proton Transfer (ESPT).

The acidity enhancement in the excited state can be seen as the consequence of a charge transfer. It was first described by Weller[57] as a charge transfer from the O atom (or the proton donor group) to the ring which makes it a better acid. On the other hand, calculations by Hynes et al.[58] have shown that the anion is stabilized in the ES and makes it a worst base instead of a better acid. In 2003, calculations done by Domcke et al.[59] have shown that the increase of the acidity is due to a non-adiabatic interaction of the $^1\pi\pi^*$ and $^1\pi\sigma^*$. The $^1\pi\pi^*$ potential energy crosses $^1\pi\sigma^*$, which induces a stabilization because of the lower energy and allows the proton to be removed. They observed that the $^1\pi\sigma^*$ state has a charge transfer character.

Absorption and fluorescence spectra of photoacid molecules are useful to determine the excited state proton transfer properties. Thus, a red shift of the conjugated base absorption and emission compared to its acid is a signature of ES(I)PT and evidences a stronger acid in the excited state than in the ground state (Figure 3−1). A Förster cycle calculation gives a good approximation of the pK_a^* in the ES. The pK_a^* can be calculated from the fluorescence spectra of the acid and base forms of the studied molecule (equation 3.6). Here, $h\nu_A$ and $h\nu_{AH}$ are the energies of the electronic transitions between the ground and the excited states of the base and acid forms respectively, R is the gas constant and T the temperature in Kelvin. However, it is important to keep in mind that the obtained pK_a^* should only be taken as an approximate value because many ESPT are competing with other non-radiative processes. Figure 3-1 presents the general scheme of the ESPT; we can see that the proton transfer rate of the forward and backward processes, k^*_{pt} k^*_{-pt}, are not the only processes involved, but fluorescence and non-radiative dissipation energy from the excited acid and base are also part of the

mechanism. Molecules such as hydroxyarenes also present radical formation from the homolytic breaking of the OH as well as quenching induced by proton transfer. The pK_a* estimation of hydroxyarenes gives large error because of the numerous parallel non-radiative channels, but it gives a reasonable value for naphthols and phenol derivatives because they present less non-radiative channels.[60]

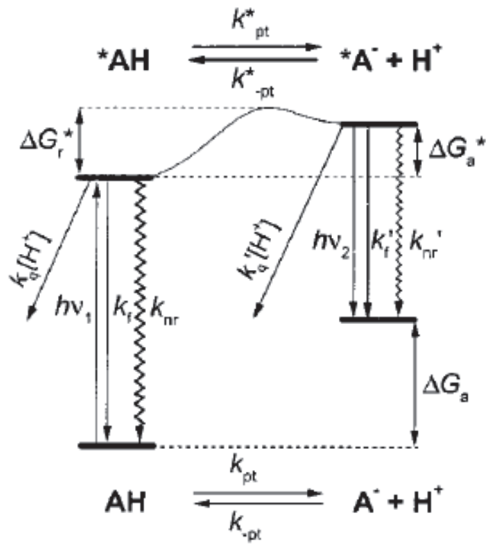

Figure 3-1: Excited state relaxation of photoacids. Figure from ref. 60.

$$pK_a{}^* - pK_a = \frac{h\nu_A - h\nu_{AH}}{2.3RT} \qquad (3.6)$$

2-naphthol for example, exhibits a pK_a* of about 7 units smaller than its GS pK_a (pK_a*= 2.8 while pK_a is 9.5).[61] The proton transfer energy barrier in the excited state is generally very much decreased compared to the GS barrier and allows fast PT, either through the small energy barrier (barrier tunneling), or through a conical intersection. Sobolewski and Domcke[59,62] have demonstrated by ab initio calculations that several aromatic molecules undergo a conical intersection in their excited state, allowing proton or hydrogen atom transfer. As an example, phenol-ammonia clusters, according to these calculations, exhibit a potential energy crossing between the $^1\pi\pi^*$ and the $^1\pi\sigma^*$ state, resulting in low activation energy for the proton transfer (Figure 3−2 b). For phenol-water clusters on the other hand, the potential energy crossing is located at a higher energy (Figure 3−2 a), explaining

why ESPT has been experimentally observed for the phenol-ammonia cluster, but not for phenol-water clusters.[63,64]

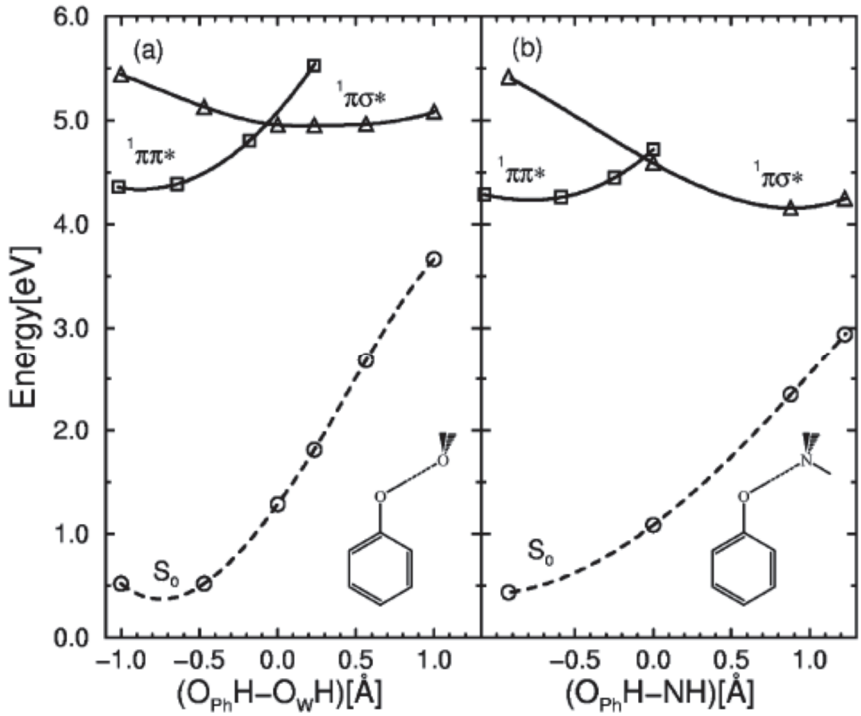

Figure 3-2: Calculated Potential energy of phenol-water (a) and phenol-ammonia (b) representing the hydrogen transfer reaction. Figure from ref. 62.

For ESPT to solvent, the solvent naturally is a key element for the rate of proton transfer. Since the solvent acts as the proton acceptor (base) a polar solvent will increase the k_{ESPT} compared to a less polar one. The duality property of water as a moderate proton acceptor, and a strong proton donor makes it an appropriate solvent for proton transfer reaction because water will solvate both the proton and the anion.[60] Changing solvent from water to alcohol often shows a slow down or a complete stop of the proton transfer. Figure 3−3 shows the influence of water content on the fluorescence emission of 1-propyl-2-naphthol (PN). When the solution contains only MeOH, only the fluorescence band of the neutral species is present around ~360 nm showing that no ESPT happens. When the water content increases a red-shifted band corresponding to the anionic form of PN arises.[65] This

shows that proton transfer occurs to the water molecules. ESPT to alcohol has been observed for strong photoacids such as 5,8-dicyano-2-naphthol (DCN2), which has a pK_a* of -4.5.[60,66]

For naphthol, the ESPT is guided by pre-existing hydrogen bonds (HB) in the GS, though solvent rearrangement in the ES is often preceding the PT itself. Agmon[61] showed that HBs in the ES provide higher stabilization of the molecule than hydrogen bonds in the GS. Thus, solvent relaxation and rearrangement are important elements in ESPT that can limit the k_{PT} especially for fast ESPT, in particular the solvation of the anion is a key factor. Slower proton transfer reactions, on the other hand, are more influenced by covalent interactions.[61] Isotope substitution usually decreases the k_{PT}, and ESPT is more sensitive to deuterium substitution than ESIPT. Based on the work of Bell[67,68], the proton tunneling through a barrier is evidenced by a large kinetic isotope effect (KIE), as well as a peculiar k_{pt} dependency on temperature (concave Arrhenius plot). A small KIE for ESPT to water shows that the proton transfer is more controlled by hydrogen bonds[61] and less by proton tunneling. In addition, it has been observed[69] that strong reversibility of the photoacids proton transfer is associated to a KIE = 3.

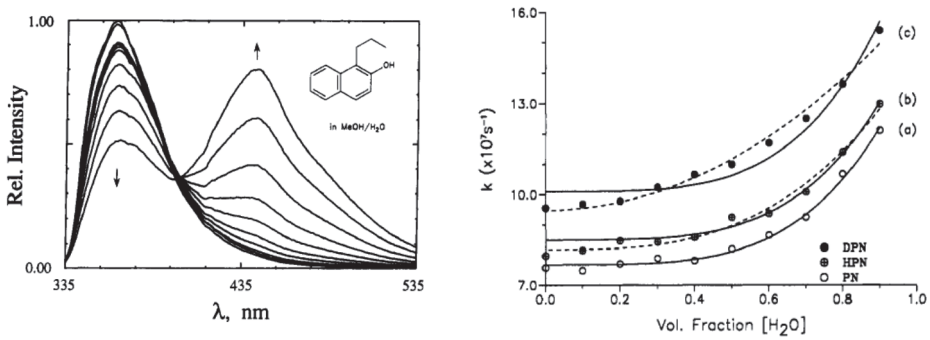

Figure 3-3: Effect of water content in methanol solution on the steady state and time-resolved fluorescence emission, of 1-propyl-2-naphthol (PN). Left panel arrows show the trend of emission upon increasing water content from 10 % to 90 %. Right panel shows the total fluorescence rate constantas a function of water fraction, PN data are represented by the open circles (curve (a)). Figure are from ref. 65.

ESPT depends on many factors, solvent as described above, but also temperature, pressure, deuterium substitution, complex formation, etc. ESPT has been studied for more than half a century and several theories have been developed to explain the role of the solvent in the process. An early model was developed by

Robinson[70], who demonstrated that in order for the ESPT to happen a cluster of water molecules need to solvate the proton. He showed that the cluster must contain four water molecules for the reaction to occur, but more recently it was shown that the number of water molecules needed to solvate the proton is dependent on the pK_a* of the photoacid.[61] Pines and Fleming[71] established, as for the proton dissociation in the ground state, a correlation between the rate of the ESPT and the pK_a. Agmon and Huppert[72,73] postulated that the kinetics of the proton transfer reveal the number of hydrogen bonds breaking and forming in the process. Hynes[74] and coworkers developed a Landau-Zener model predicting the rate of PT. This model also takes into account the transition from the adiabatic to the non-adiabatic transition regime of the process. This approach also describes the temperature dependence of the PT rate, but it can give limited results when there is strong interactions with the environment.[75]

The mechanism of the proton transfer is not a one step process; it can be viewed as a serie of elementary processes occurring from the femtosecond to the millisecond timescale. A general picture of the process can be given as follows: the excitation of the molecule is followed by an electronic redistribution leading to the change of pK_a*; hydrogen bonds are rearranged near the proton donor group, which help the proton dissociation; if a barrier is present on the potential energy surface (PES), geminate recombination may occur; and finally quenching of the excited state is observed.[61] Several groups[76-78] have observed these multiple steps in the proton dissociation process, for example Huppert et al.[77] studied ESPT from 8-hydroxypyrene 1, 3, 6 trisulfonate (HPTS) to water. The following three step process was proposed to explain the whole proton dissociation reaction: the first step is to form a contact ion pair or radical, the 2nd step involves a further dissociation influenced by the solvent and the final 3rd step is the actual dissociation assisted by diffusion. The mechanism is presented in the following equation,[77]

$$\mathrm{ROH^* + H_2O} \overset{\text{step one}}{\underset{k'_r}{\overset{k'_{PT}}{\rightleftharpoons}}} \underbrace{[\mathrm{RO^-{*}\cdots H_3O^+}]_{(r=a)}}_{\text{contact ion pair}} \overset{\text{step two}}{\underset{k_r}{\overset{k_{PT}}{\rightleftharpoons}}}$$

$$\underbrace{[\mathrm{RO^-{*}---H_3O^+}]_{(r=a)}}_{\text{separated ion pair}} \overset{\text{step three}}{\underset{}{\overset{DSE}{\rightleftharpoons}}} \mathrm{RO^-{*} + H_3O^+}$$

Experiments on photoinduced proton transfer from pyrianine to solvent[78] observed two ultrafast steps before the actual proton transfer step of 87 ps. The authors attributed the first 300 fs step as a fast solvation process of the locally excited state of the acid, then the locally excited state relaxes to an intermediate species in 2.5 ps before the PT happens.

Excited state intramolecular proton transfer (ESIPT) often occurs from an oxygen donor to a nitrogen acceptor, but the acceptor can also be oxygen. Few cases where the acceptor is a carbon atom and the donor a nitrogen have also been observed.[79] The resulting photoproduct of ESIPT is the corresponding tautomer form of the molecule, and unlike ESPT the product formed is globally neutral. Arnaut defined ESIPT[79] as the intrinsic proton transfer from the donor to the acceptor. By this definition we understand that the pre-existing HB between the donor and the acceptor group in the ground state is the leading element of the k_{ESIPT} and the solvent can prevent direct ESIPT and can lead to ESPT. There are many similarities between the ESIPT and ESPT processes. As previously mentioned, the ESIPT reaction also presents a strong red-shift of the tautomer absorption or fluorescence spectrum as compared to the normal species. A fluorescence rise time of the product form and the decay of the original species describe the fluorescence kinetics of the ESIPT. Similarly to ESPT, ESIPT can be really sensitive to the solvent. The environment is a good energetic probe for the overall mechanism of ESIPT.

Zewail et al.[80] described the process of ESIPT by three types of PES that can be: 1) Barrierless ESIPT 2) tunneling through a low energy barrier and 3) tunneling through a high energy barrier. Depending on the PES the ESIPT can exhibit different responses to solvent and temperature, as well as being characterized by a large range of k_{ESIPT}. The different PES profiles can be examined by deuterium substitution; the presence of a fluorescence band of the normal form is also a signature of an energy barrier between the two species.

Methyl salicylate (MS) is an example of barrierless ESIPT. Deuterium substitution has no effect on the kinetics and the rate of the proton transfer has been observed to be as fast as 60 fs by Zewail et al.[80], which makes this ESIPT reaction much faster than ESPT. The barrierless process is evidenced by the absence of a KIE, as well as the absence of the fluorescence band of the normal species. Tunneling through a barrier is associated with a KIE, since tunneling is sensitive to mass change. The absence of emission from the original excited state species is generally a sign of a favorable process with a low energy barrier. 2-(2'-

hydroxyphenyl)-5-phenyloxazole (HPPO) has a k_{ESIPT} of $(220\ fs)^{-1}$, and only the fluorescence of the tautomer species is detectable. Its PES is an asymmetric double well[81] and a strong pre-existing hydrogen bond in the GS can be a reason for the fast k_{ESIPT}. The intervention of polar solvent able to create hydrogen bonds with the proton donor group can change the ESIPT into localized ESPT, and allow the observation of the normal fluorescence. Fluorescence of both species is often observed for slow ESIPT, and evidences the presence of a rather large barrier.

To close the cycle of the ESPT reaction, the last expected step is the recombination. In time-resolved fluorescence measurements recombination shows up as a long non-exponential tail on the order of ns. GS recovery can be reached through either recombination (eq. 3.7) - homogeneous or geminate - or a quenching reaction (eq. 3.8). Homogeous recombination is the result of recombination with the proton of the surrounding solvent while geminate recombination occurs with the same transferred proton.

$$R^*O^- + H^+ \rightarrow R^*OH \qquad (3.7)$$

$$R^*O^- + H^+ \rightarrow ROH \qquad (3.8)$$

Weller[82] has first shown the homogenous reversibility of ESPT by fluorescence titration, Laws and Brands[83] performed time-resolved measurements at low pH on 2-naphthol and found a bi-exponential decay, attributed to the backward reaction. Webb et al.[84] proposed a back reaction with the dissociated proton and the part of the molecule where the electron density is the highest. This reaction would lead to a fast recovery of the acid GS. Recombination at neutral pH can occur with the geminate proton and usually happens within nanoseconds after the proton ejection and is a non-exponential process.[85] Non-exponential fluorescence on the long timescale is a signature of geminate recombination. Agmon et al.[61,86-88] have developed a diffusion based model to describe the excited state geminate recombination. They have shown that in the general case when the acid and the base have different lifetimes, and when the excited acid decays faster than the base (most common for ESPT to solvent), the base is the form with highest ES concentration. Diffusion has time to take place and the obtained decay is not exponential but follows an asymptote in the long range time of $t^{-3/2}$.

All these studies demonstrate that excited state proton transfer reactions are complicated and are not yet fully understood. ESPT/ESIPT are multistep processes controlled by both intramolecular and intermolecular properties and processes.

Though the process is a common chemical reaction it is difficult to paint a general picture of the mechanism. Excited state proton transfers are the main relaxation process of several aromatic molecules of chemical or biological relevance, containing an alcohol group. We believe our work demonstrates that ESPT/ESIPT is the main UV photoprotection and dissipation channel for eumelanin and its building blocks, as it will be discussed in the next chapters.

4- From Eumelanin Monomers to Polymer

The main difficulty in the study of the melanin pigment is its chemical heterogeneity and the loss of solubility in aqueous solvent going from monomer to polymer. The solubility issue will be addressed in the second part with the oligomers study. The chemical heterogeneity is bypassed by the study of synthetic samples and the bottom up approach from monomer to polymer of one building block. This method allows us to identify the specific contribution of each eumelanin constituents and to reconstruct the optical properties step by step.

4.1- Monomers

The first part of this chapter focuses on the monomers study in solution.

Eumelanin is made from indole derivatives. Indole has been extensively studied over years.[89-94] It is the main chromophore of tryptophan, an important molecule used to investigate the protein function. As simple as the indole structure is, its photochemistry is complicated and relies on several processes. Indole absorbs around 280 nm and emits around 340 nm. Its spectral properties are highly sensitive to the environment, especially to the solvent polarity.[89]

UV-excitation of indole results in a series of processes, ranging from ionization and intersystem crossing to radical cation formation accompanied by solvated electron in aqueous solvent.[89,90,93,95,96]

To understand the mechanisms and products of UV-excitation of the eumelanin pigment we have studied three different indole derivatives monomers, ICA, DHICA and DHI (refer to Figures 4−6 and 1−2 for the structures). As described earlier, DHICA and DHI are the two mains precursors of eumelanin. Their photochemistry is essential to understand the functionality of each precursor and why DHICA seems to be the prevalent motif of natural eumelanin. The study of

ICA helps us give insight into the process involving carboxyl groups in the UV deactivation process.

4.1.1- Paper I: Photochemistry of ICA

One of the most fundamental building blocks of eumelanin is the DHICA molecule; photoprotection properties of DHICA are believed to be stronger than of DHI.[97] The main difference between the two molecules is the presence of the carboxyl group in the C2 position of DHICA. In order to investigate the role of the carboxyl group in eumelanin, *ab initio* calculations and experiments were combined to get a picture of the photochemistry of indole-2-carboxylic acid (ICA) in aqueous solution, since ICA contains the least number of functional groups compared to DHI and DHICA.

ICA was studied in acidic and neutral conditions to compare the anionic and the neutral forms of the molecule, referred as ICA-A and ICA-N, respectively. The pK_a of the carboxyl group was measured to be 3.69[98], meaning that at pH 7, 99 % of the molecules are anions. At pH 2.5, 94 % are fully protonated, and the remaining 6 % are in the anionic form. The *ab initio* calculation included three water molecules to simulate the solvent environment. Due to the possible hydrogen bonds formed with the molecule, three water molecules were determined to be the minimum to describe the solvent effects. The two oxygen atoms from the carboxyl group as well as the nitrogen atoms of the NH group are the three possible atoms to be involved in hydrogen bonding as either acceptor or donor of a proton.

4.1.1.1- Anionic species studied at pH 7

The absorption spectrum of ICA-A exhibits one minor band around 4.1 eV, a main one at 4.32 eV and strong absorption above 5 eV, Figure 4−2. The fluorescence spectrum has a main band at 3.62 eV and a minor one at 3.1 eV, Figure 4−1 (A). The presence of the 3.62 eV band, both in the fluorescence spectrum of ICA-N and ICA-A is an indication that this band belongs to the ICA-A, 6 % of the anionic form is present at pH 2.5. Only one fluorescence lifetime of 4.9 ns was measured throughout the emission wavelengths, Figure 4−1 (B).

In the ground state, several stable A-keto forms were calculated, differing from each other through the position of the water molecules. One of these geometries is lower in energy by 0.1-0.2 eV than the rest and taken as the ground state

equilibrium geometry. In the excited state (ES), two stable minima are computed the $^1\pi\pi^*$(A-keto) with the proton positioned on the indole nitrogen, and the $^1\pi\sigma^*$(A-enol) with the proton on the carboxyl group. The A-enol is energetically favored by approximately 0.1 eV.

The transition energies calculated for the A-keto form indicate that the 4.1 eV band is due to the transition $S_0 \rightarrow S_2$, the 4.32 eV transition corresponds to the $S_0 \rightarrow S_3$ transition, and the bands above 5 eV are due to transitions to higher singlet states.

Direct excitation of the ground state A-keto form through the S_2 or S_3 transitions leads to internal conversion to the lowest $^1\pi\pi^*$(A-keto) state. The $^1\pi\sigma^*$ state of the A-enol form positioned just below the $S_1(\pi\pi^*)$ state of the A-keto form suggests the possibility of ESIPT from the indole to the carboxylic group.

The calculations also predict strong emission from the $^1\pi\pi^*$(A-keto) state at 3.78 eV, in good agreement with the 3.62 eV fluorescence found experimentally; the small difference between calculated and experimental values is most likely due to the 0.3 eV overestimate usually present in the calculations.[99]

The fluorescence lifetimes measured experimentally indicate that the ESIPT probably occurs on the nanoseconds timescale, suggesting that this dissipation channel is a minor one. The weak emission band at 3.1 eV could come from relaxation from $^1\pi\sigma^*$(A-enol) state.

Schematic of the ES mechanism is illustrated in Figure 4−1 (right panel).

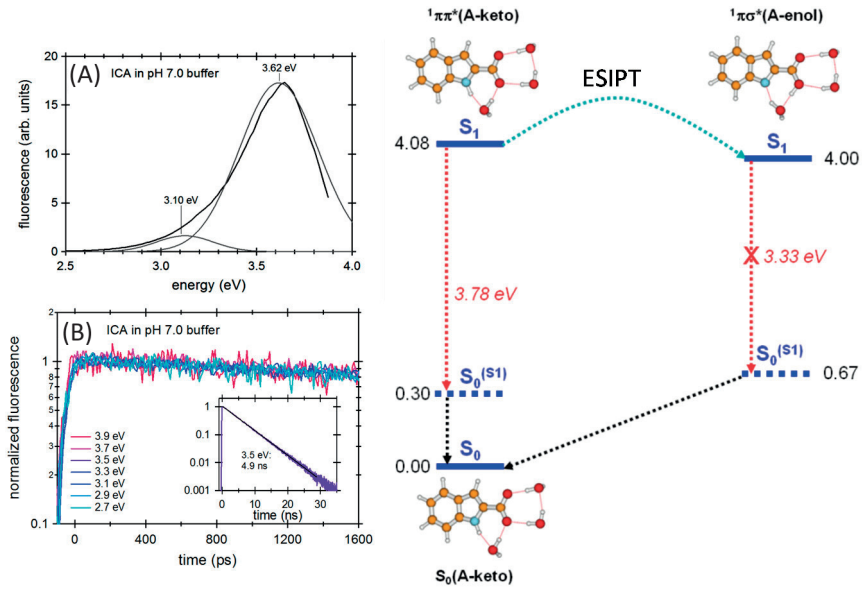

Figure 4-1: Left panel, graph (A) shows the experimental steady state fluorescence spectrum of ICA in pH 7 phosphate buffer (Black) together with its spectral fit (Grey). Graph (B) shows the time-resolved kinetic traces of ICA in pH 7 buffer solution at different energies. Inset presents the time trace recorded at 3.5 eV, the fit results in a 4.9 ns decay. Right panel shows the calculated energy levels of ICA-A together with indicated ground and excited state processes.

4.1.1.2- Neutral Species studied at pH 2.5

The absorption spectrum of ICA-N (in pH 2.5) is red shifted compared to that of ICA-A (in pH 7), Figure 4−2. The maximum optical density of ICA-N is at 4.25 eV and the steady state fluorescence measurement shows two bands one at 3.62 eV, as earlier mentioned attributed to the 6 % of ICA-A and a second more intense at 3.04 eV that must originate from ICA-N, Figure 4−3 (A). The

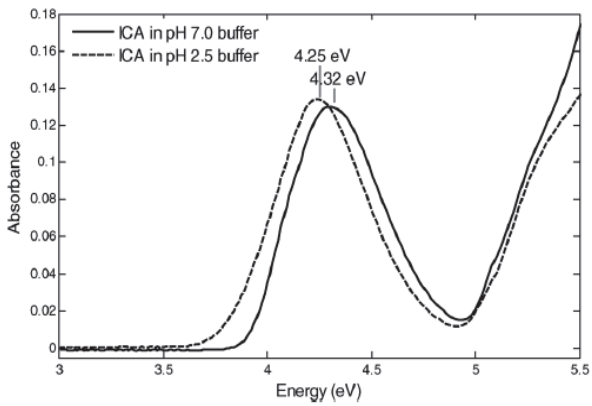

Figure 4-2: Absorption spectra of ICA-N (in pH 2.5, dashed line) and ICA-A (in pH7, solid line).

proportion of the two emission bands shows that the radiative decay is not the main dissipation channel for ICA-N, since the band attributed at ICA-A is much more intense than expected for the small 6 % fraction of the species in the GS. Time-resolved fluorescence measured two decay times, one in the blue side of the emission spectrum of 4.9 ns, which confirmed that the 3.62 eV band is the same as the one present in ICA-A. The lifetime extracted on the red side of the spectrum is 1.6 ns and assigned to ICA-N, Figure 4−3 (B).

Unlike ICA-A, ICA-N is predicted to have two stable ground state species, S_0(N-cis) and S_0(N-trans), Figure 4−3 right panel. They are protonated at both the indole nitrogen and the carboxyl group and the torsion angle of the carboxylic acid group has a 180° different twist relative to the indole plane. The two lowest transitions to the S_1 and the S_2 states of the cis and trans forms are predicted to have quite similar energies, which results in strongly overlapping absorption spectra. The transition to S_2 is predicted to have a higher oscillator strength; thus the weak red edge of the absorption band is attributed to the $S_0 \rightarrow S_1$ transition and the main absorption to $S_0 \rightarrow S_2$. Like for ICA-A, the absorption above 5 eV is expected to come from higher excited state.

The fluorescence emission from the cis and the trans excited states both are of $^1\pi\pi^*$ character and fluorescence measurement cannot distinguish them due to their very similar energy. The values found for the emission are slightly different from the experimental observation; they are a bit more overestimated than the expected 0.3 eV from the systematic error in calculation. Running different computational methods showed that the differences arise from solvent properties.

The 1.6 ns fluorescence lifetime of ICA-N, considerably shorter than the 4.9 ns of ICA-A, suggests that a radiationless process on the nanosecond timescale is competing with radiative decay of the lowest excited states of the cis and trans forms. The calculations indicate that this radiationless process could be the first step of a full or partial ESIPT of the carboxylic acid proton towards the indole nitrogen.

Schematic diagram of the relaxation process is illustrated in Figure 4−3, right panel.

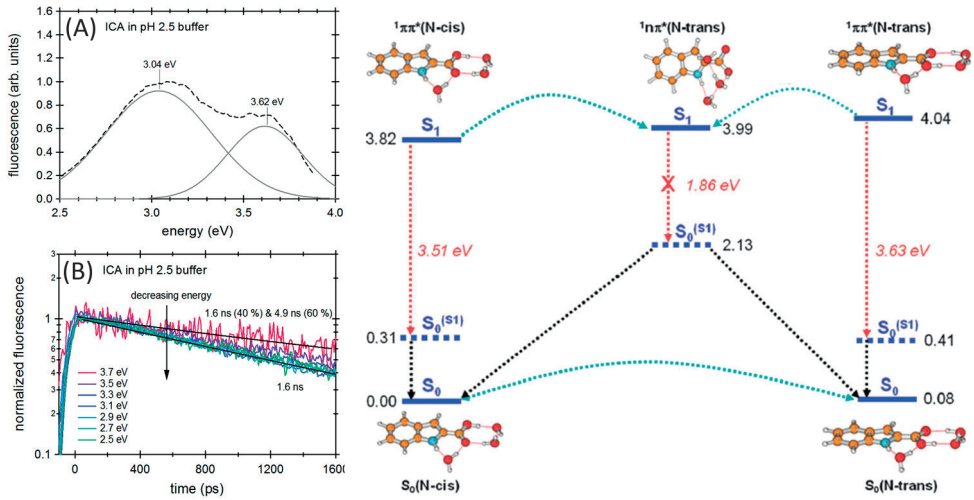

Figure 4-3: Left panel, graph (A) shows the experimental steady state fluorescence spectrum (black dashed lines) of ICA in pH 2.5 phosphate buffer together with its fit (grey solid lines). Graph (B) shows the time-resolved kinetic traces of ICA in pH 2.5 buffer solution at different detection energies, the fits (black lines) result in two components ,1.6 ns on the red side on 4.9 ns on the blue side of the fluorescence spectrum. Right panel illustrates the calculated energy levels of ICA-N together with indicated ground and excited state processes.

4.1.1.3- Conclusion Paper I

The combination of computational and experimental work was useful to understand the photochemistry after UV absorption of ICA. It is interesting to note that as expected for indole molecules, ICA is highly sensitive to pH and the carboxyl group has an important function in the photochemistry of the molecule. The UV-dissipation channel is mainly radiative for the ICA-A form, but largely non-radiative for the ICA-N form.

4.1.2- Paper II: DHICA

In comparison to ICA, DHICA possesses three groups which can exist in protonated or deprotonated state, a carboxylic acid group at C2 and two OH groups at C5 and C6 (for numbering see DHI Figure 4−10), their pK_a were measured to be 4.25, 13.2 and 9.76 respectively.[100,101] Previous studies[102,103] on DHICA have shown that the molecule is sensitive to solvent – according to the pK_a, different species will be present depending on the pH. Studies at pH 7 and pH 2.5 have shown that UV-absorption leads to different relaxation processes. At pH

7, were the main ground state species is the anionic form of DHICA (the carboxyl group is deprotonated) long fluorescence lifetimes were measured, 1.6 ns at the blue side and 2.4 ns at the red side of the fluorescence spectrum, Figure 4−6 (A). These lifetimes were attributed to the relaxation of the anionic species and to a complex formation involving DHICA and the buffer salts, respectively. In the work presented in paper II, we demonstrated that these ns lifetimes are in fact the result of a slow ESPT from the hydroxyl group to the solvent and relaxation of a photoproduct.

Previous work at pH 2.5, where the molecule is mainly in its fully protonated form showed that UV-absorption leads to the formation of a red-shifted zwitterionic species relaxing back to the ground state with a time constant of 240 ps. The zwitterion was believed to be formed via ESIPT in a sub- picosecond timescale, but the PT rate was not determined and the relaxation from the original ES was not observed with the used streak camera technique. Here we resolve the ultrafast ESIPT with the help of fluorescence up-conversion and we demonstrate the participation of solvent molecules in the proton transfer mechanism. As predicted by the previous studies of DHICA this process is indeed in the sub-ps time range.

The first step of the work in this paper was to identify the species present in a large pH range. Band analysis of the steady state absorption and fluorescence spectra was used to achieve this. The number of species present was further confirmed by time-resolved fluorescence measurements. The red shifted band of the zwitterion species was identified at 450 nm (Figure 4−4 blue curve) and present in a pH range were the neutral DHICA exists in the ground state and as known from earlier studies has a lifetime of 240 ps. At high pH a red shifted band with maximum at 416 nm is attributed to the double anion of DHICA ($DHICA^{2-}$), Figure 4−4 red curve. As expected from the pK_a of the carboxyl

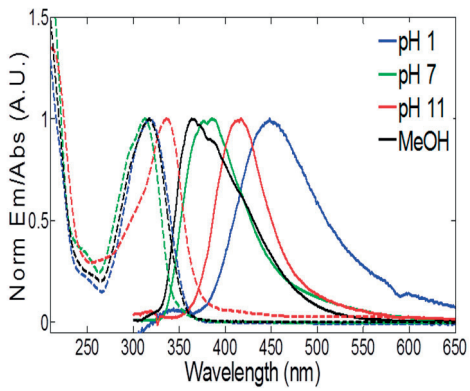

Figure 4-4: DHICA steady state absorption (dashed lines) and fluorescence (solid lines) spectra in pH 1, 7, 11 and methanol, blue, green, red and black curves respectively. Main species present at pH 1 is the neutral DHICA form, the ground state species at pH 7 is mainly the $DHICA^-$, and the GS species at pH 11 is mainly the $DHICA^{2-}$

group the main species present in the pH range 1 to 11 is the monoanion; its fluorescence emission maximum is at ~ 380 nm, Figure 4−4 green curve. DHICA in MeOH has a single fluorescence band with a maximum peaking at 360 nm and a lifetime of 3.5 ns, Figure 4−4 black curve.

4.1.2.1- Neutral DHICA

The occurrence of the DHICA zwitterion strongly suggests the ESIPT reaction initiated by UV-absorption. Fluorescence up-conversion (FU) measurements on DHICA at pH 2.5 exhibit an ultrafast decay. The main part of this decay can be fitted with a 300 fs component (Figure 4−5 (A)), but it also contains a minor 1-ps component, as well as a constant component attributed to the 240-ps zwitterionic fluorescence decay measured with the streak camera. In MeOH no such fast decay is present. The fluorescence profile shows a rather long relaxation of 3.5 ns (Figure 4−5 (B)) accompanied with a weak ps component. We observed the corresponding ps rise on the red side of the emission spectrum. This kind of behavior is typical for excited state solvation dynamics, and the lifetime corresponds to the value found in literature for MeOH.[104] We believed the ps decay in aqueous solution is also a signature of solvation dynamics;[105] Fleming and Pines, for instance, showed that solvation dynamics in water typically occurs on the 1-10 ps timescale.

We attribute the 300 fs decay to the ESIPT process where a proton is transferred from the carboxylic acid group to the indole nitrogen. The experiments show that water molecules are needed in order for the process to happen, thus we can consider the process as a solvent assisted ESIPT; in that respect it resembles the type of proton transfer in some proteins mediated by a solvent wire from a donor to an acceptor group. It seems that intramolecular HBs are important to get a rapid and efficient transfer. The ESIPT could also be viewed as similar to that in substituted naphthol studied by Tolbert and coworkers[106], who showed the importance of HBs with the water solvent for ESPT to happen.

Schematic representation of the relaxation process of neutral DHICA is illustrated in the right panel of Figure 4−5. The lifetimes and the emission wavelengths associated to the different species are also indicated.

These observations are also in agreement with the calculations performed for ICA-N where ESIPT seems to be possible with the presence of a water molecule.

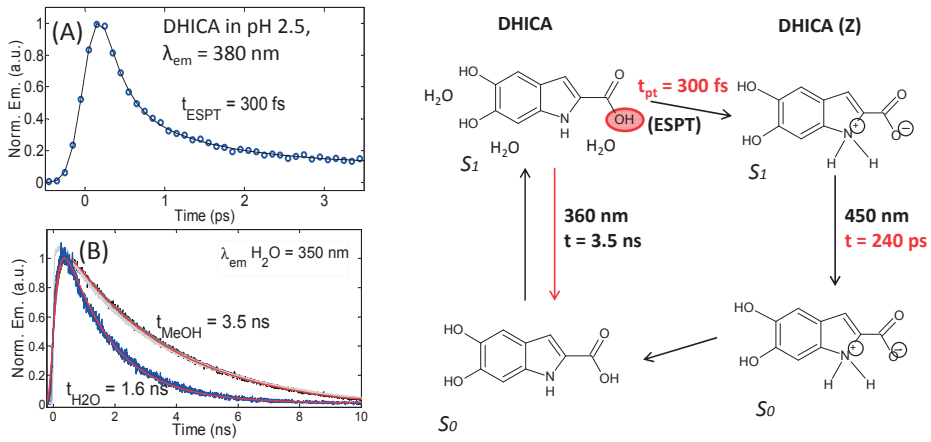

Figure 4-5: Left Panel, graph (A) displays the emission decay of DHICA in pH 2.5 at 380 nm emission wavelength together with its fit, giving a 300 fs lifetime. Graph (B) shows the measured emission decays of DHICA in pure water at 350 nm (blue) and the emission decay traces of DHICA in methanol recorded between 400 and 550 nm (black to grey scale). The fits (red traces) resulted in a lifetime of 1.6 ns and 3.5 ns in water and MeOH respectively. Right panel presents neutral DHICA excited state relaxation scheme after UV excitation in acidic condition. Lifetimes and emission wavelengths for the different species are also indicated.

4.1.2.2- Monoanion DHICA⁻

The previous work at neutral pH suggested a complex formation with the buffer salts as explanation to a 2.4 ns fluorescence lifetime of $DHICA^-$. However, it is known that buffer can favor ESPT reactions to the solvent. Moreover, as described above, calculations performed by the Meredith group suggest proton transfer from the OH groups to the solvent. The nanosecond timescale decays observed are typical for ESPT to solvent for medium strengths photoacids such as naphthol. Such photoacids usually exhibit proton transfer in aqueous solution, but not in alcohols. Time-resolved fluorescence measurements of DHICA in water/MeOH mixtures, in the blue side of the emission spectrum shows a fluorescence decay dependent on the MeOH concentration. The observed fluorescence lifetime goes from 3.5 ns in neat MeOH to 1.6 ns in neat water (Figure 4−5 (B)). FU measurements also show a 1-ps decay attributed to solvation dynamic as for DHICA at pH 2.5. We believe the solvent dependence and the presence of the double anion species at lower pH strongly support the ESPT to solvent as the main channel for UV-absorption dissipation and that ESPT stops, or significantly slows down in MeOH.

The ESPT results in the formation of $DHICA^{2-}$. The double anion emits at 500 nm and has a lifetime of 2.4 ns, Figure 4−6 (A).

The 1.6 ns decay measured for $DHICA^-$ at pH 7 (Figure 4−6 (A)) represents the sum of the relaxation from the original ES back to ground state, as well as the proton transfer. Assuming that the intrinsic relaxation lifetime of $DHICA^-$ in water is the same as in MeOH we can determine the k_{ESPT} to be $(2.5\ ns)^{-1}$.

Moreover a Förster cycle calculation predicts a $\Delta pK_a = 5$; thus, DHICA is not a strong photoacid. The rate of the ESPT is of the same order of magnitude as previous ESPT rates observed for similar molecules. Similar measurements performed on ICA, where the two hydroxyl groups are missing, also support the ESPT mechanism since ICA in different water/MeOH contents do not show any solvent dependence of the 400 nm emission decay, Figure 4−6 (B).

A scheme of the relaxation pathways of $DHICA^-$ the lifetimes and emission wavelengths associated to the different species involed is presented in Figure 4−6 right panel.

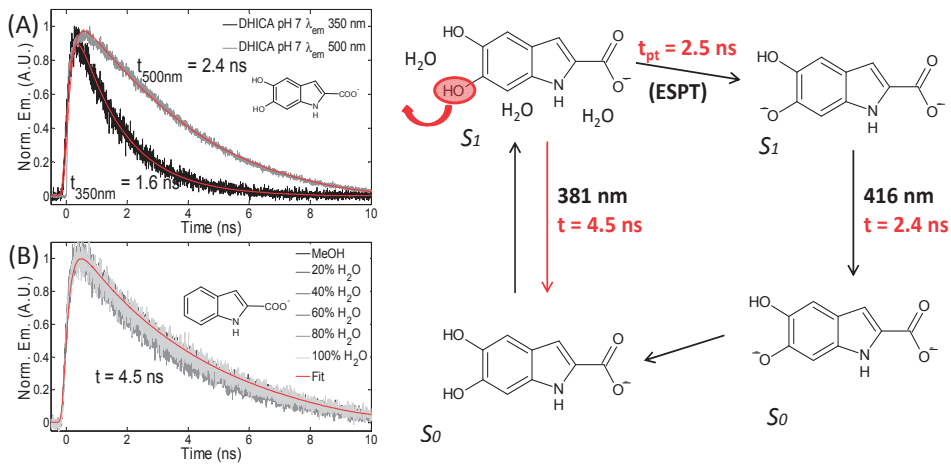

Figure 4-6: Left panel, graph (A) shows the emission decays of $DHICA^-$ in pH 7 measured at 350 nm (black curve) and 500 nm (grey curve) together with their fits (red curves) resulting in 1.6 ns and 2.4 ns lifetimes, respectively. Graph (B) shows the emission decays of ICA in different Water/MeOH mixtures recorded at 400 nm. Right panel illustrates $DHICA^-$ excited state relaxation pathways after UV excitation.

4.1.2.3- Conclusion Paper II

The work presented in paper II demonstrates excited state intramolecular proton transfer from COOH to NH for neutral DHICA, and shows that the process is ultrafast with a time constant of ~300 fs. The anionic form of DHICA also relaxes through an excited state proton transfer process, but in this case excited state proton transfer to the solvent on a much slower timescale.

4.1.3- Paper III: DHI

DHI is the least studied of the two main eumelanin building blocks, mainly due to its degradation in aqueous solution enhanced by light exposure. Because DHI does not possess the carboxyl group, its occurrence at epidermis pH is believed to be mainly protonated in GS. Previous time-resolved pump probe experiments showed that the deactivation mechanism after UV-absorption is characterized by two relaxation channels, a nanosecond one believed to be ESPT, and a faster one 100-ps process attributed to cation radical formation.[107] Calculations in the gas phase performed by Sobolewsky et al.[108] suggested that a stable photoproduct with a strong absorption in the visible region is formed after UV-excitation. The photoproduct is the consequence of a hydrogen transfer from the OH group at C5 to the carbon C4 (for numbering see Figure 4−10). The migration of the H-atom initiates a fast tautomerization of the molecule in the excited state.

The new investigation of DHI presented here brings evidence of an ESPT channel as the main excited state dissipation mechanism. The mechanism was proved by the measurement of DHI in water/methanol mixtures and of DHI in deuterated buffer. The analysis of two DHI derivatives also adds information on the relative contributions of the two OH groups to the overall ESPT process.

An excitation wavelength dependence of the fluorescence is revealed, and by comparison to emission measured for well characterized DHI-dimers, assigned to dimers and higher oligomers of DHI formed as a photoproduct in the course of measurements.

In the experiments, steady state absorption and fluorescence were measured and two absorption bands defined the absorption profile of DHI in buffer, Figure 4−7 (A). The fluorescence spectrum presents two bands with excitation wavelength dependent intensities: when the excitation is below 320 nm the main emission band is at 340 nm and when the $\lambda_{exc} > 320$ nm the main emission is a broad band

peaking at 380 nm. Emission decay of the blue band was measured to be ~110 ps and the red band has a lifetime of ~1.6 ns, Figure 4−7 (B).

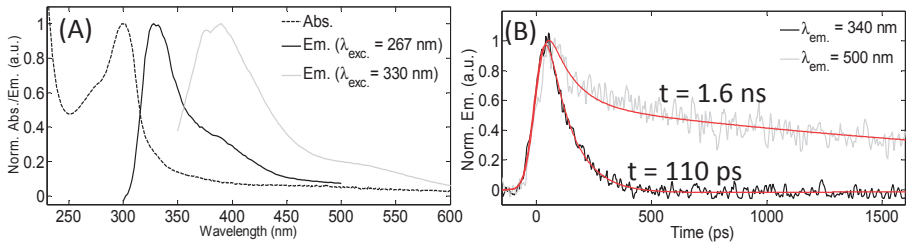

Figure 4-7: Graph (A) shows steady state absorption (dashed line) and fluorescence spectra upon 267 nm (black solid line) and 330 nm excitation (grey line) of DHI in pH 7 phosphate buffer. Graph (B) shows the fluorescence kinetics of DHI at pH 7 and 340 nm (black curve) and 500 nm (grey curve) detection upon 280 nm excitation, together with fits resulting in 110 ps and 1.6 ns lifetimes.

4.1.3.1- Evidence of the ESPT

As for $DHICA^-$ experiments in water/MeOH solvent mixtures show a strong dependence of the emission decay rate on water concentration, going from ~103 ps in neat water to ~2.2 ns in neat MeOH, Figure 4−8.

The similar behavior of DHI and $DHICA^-$ strongly suggests ESPT as one of the relaxation channel, and that ESPT stops in alcohol solution. However, the observed ESPT in DHI is much faster than that of DHICA. Quantum chemical calculations helped to rationalize the observed difference between DHI and DHICA. The calculations show a much higher energy barrier for ESPT of the complex $DHICA^-$/water than for DHI/water, 0.73 and 0.44 eV respectively. Both DHICA/MeOH and DHI/MeOH have a rather high energy barrier, 0.78 and 0.53 eV respectively, explaining the

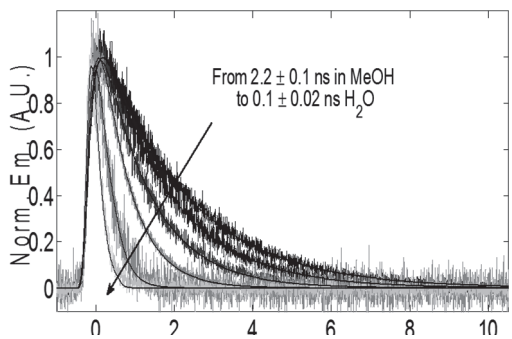

Figure 4-8: 350 nm emission decays of DHI in different water/MeOH mixtures together with their fit decreasing from 2.2 ns in neat MeOH to 0.1 ns in neat water.

inhibition of the proton transfer in methanol. As expected for an ESPT reaction, DHI in pD 7 exhibits a slower decay than DHI in pH 7 (Figure 4−9 (A)), a KIE of 3 is observed, a typical value for a reversible proton transfer reaction.

We believe that the experiments as well as the calculations show that absorbed UV-energy by DHI, similarly to $DHICA^-$, is dissipated through ESPT to solvent. The pK_a^* is difficult to measure because the spectrum is disturbed with the red shifted emission, that we attribute to a degradation product. We can assume that the ΔpK_a^* is at least of the same order of magnitude as for $DHICA^-$ (about 5), or larger taking into account the much shorter emission lifetime of DHI compared to $DHICA^-$. The study of two DHI derivatives helped us to assign the active groups in the proton transfer mechanism.

4.1.3.2- Groups involved in the ESPT

Previous calculations[108] in the gas phase presented a model where the hydrogen of the hydroxyl group in C5 position was the main actor after UV-absorption. If the hydrogen in C5 is the main actor of the ESPT we expect to see large differences in the fluorescence measurement of the 5M6HI derivative (structure is plotted in graph (B) of Figure 4−9), where the hydrogen of the C5-OH group has been replaced by a methyl group. The experiments show that the fluorescence response of the derivative is similar to that of DHI. Both have a decay on the 100-ps timescale in buffer, which slows down to ~3 ns in methanol, Figure 4−9 (B). The KIE is ~ 3 for both molecules. We believed that 5M6HI also undergoes ESPT after excitation. The lifetime of 5M6HI is slightly longer than for DHI, 160 ps vs. 103 ps. If we assume that the intrinsic relaxation lifetime of 5M6HI is the same as the lifetime obtained in MeOH, we can deduce the ESPT rate to be $5.9 \times 10^9\ s^{-1}$. The similar absorption and fluorescence steady state spectra of DHI and 5M6HI suggest that the light induced species are essentially the same. The difference in the excited state decay between DHI and 5M6HI and the similar pK_a values of the two hydroxyl groups, suggest that both OH groups are involved in the ESPT for DHI. Assuming that the k_{ESPT} for the C6-OH in DHI is the same as for 5M6HI the k_{ESPT} from the C5-OH is estimated to be $3 \times 10^9\ s^{-1}$.

As discussed above, the blue side of the DHI emission was identified to be due to ESPT (Figure 4−9 right panel presents the ESPT channels). In the last part of paper III we show that the red band emission is due to degradation of DHI and formation of dimers and higher aggregates.

4.1.3.3- Red band emission

During the measurements in MeOH and for the DHI derivative (5M6HI) we observed that the emission at 380 nm was less pronounced than for DHI in buffer. The methylation of the OH-group at the C5 position is known to inhibit polymerization at C4, which is one of the favorable spots for dimerization. We also observed that the intensity of the 380-nm band tends to increase with time and irradiation. All this made us believe that the red band fluorescence is the signature of DHI impurities or degradation.

Comparison of the 380-nm DHI emission, steady state and time-resolved, with that of DHI dimers and polymer shows that both spectral position and lifetime coincide really well. DHI dimers emit around 380 nm and have a ns lifetime. Moreover, measurement in the extreme red part of the emission spectrum shows a 3-ns decay, similar to that observed for a DHI polymer. Additional proof of DHI oxidation and dimer formation, is the result for the derivative N-MeDHI. It was shown in the paper that methylation of the indole nitrogen does not have a great effect on the photochemistry of DHI. It shows similar behavior, but different excited state lifetime, attributed to the different electron density due to the methyl group on the N-atom. Like for DHI the red-shifted emission of N-MeDHI is spectrally and temporally similar to that observed for the corresponding dimer (contrary to DHI, NMe-DHI only has one possible dimer configuration).

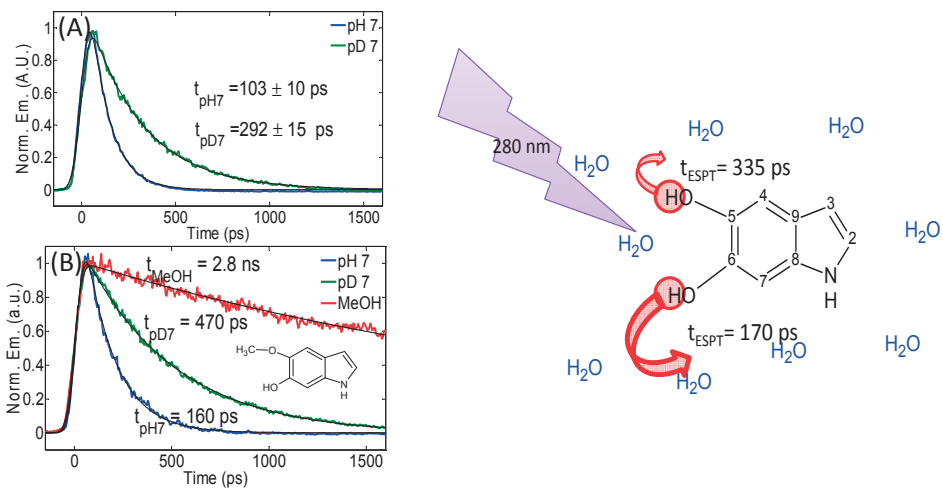

Figure 4-9:. Left panel, Graph (A) shows the emission decays of DHI in both pH 7 (blue) and pD 7 (green) measured at 350 nm together with their fits resulting in 103 ps and 292 ps lifetimes, respectively. Graph (B) shows emission traces of the derivative 5M6HI in pH 7 (blue), in pD 7

(green) and in MeOH (red) at 350 nm. The lifetimes obtained after fitting are 160 ps, 470 ps and 2.8 ns respectively. Right panel, DHI excited state relaxation mechanism after UV excitation.

4.1.3.4- Conclusion Paper III

This work is the first to experimentally observe ESPT for DHI in solution. We have evidence that the main channel of excited state decay is ESPT, and that both hydroxyl groups are involved in the process. In addition the excitation wavelength dependence and the red emission band were explained to be due to oxidation products of DHI in solution.

4.1.4- Monomers Conclusion

The UV-absorption dissipation mechanism was studied by steady state and time-resolved fluorescence spectroscopy of the two main eumelanin building blocks. As expected for indoles their photochemistry is strongly dependent on the environment. We have shown that the main dissipation channel in aqueous solution is excited state proton transfer and excited state intramolecular proton transfer. Though both molecules present the same excited state relaxation process, the timescale of the UV deactivation is different. At low pH where DHICA is in its neutral form with the carboxylic acid group protonated, ultrafast fluorescence up-conversion measurements showed that a solvent mediated ESIPT from the COOH group to the NH group occurs with a time constant of 300 fs. At epidermis pH between 4 and 6[109] DHICA and $DHICA^-$ are expected to be present, while DHI is found in its protonated form. Both molecules are medium strength photoacids with rather slow nanosecond timescale k_{ESPT} in aqueous solution. The absence of ESPT in alcohol solution supports the medium range pK_a^* as well as the need of hydrogen bonding with water molecules already in the ground state. The much faster rate of ESPT from the hydroxyl groups of DHI compared to $DHICA^-$ suggests that the pK_a^* might be smaller for DHI than $DHICA^-$, i.e. that DHI in the excited state is a stronger photoacid than $DHICA^-$.

The work on the monomers is a basis for understanding the photochemistry of the larger oligomers.

4.2- Oligomers and Polymer

The study of synthetic or natural polymers and oligomers in solution is rather complicated due to the loss of solubility when the chain elongates. Already from the dimer level we observed a poor solubility for both DHI and DHICA. The polymer forms aggregates difficult to dissolve in solution. In order to study eumelanin in aqueous solution a solubilization method had to be developed. Paper IV compares two methods to address this issue, in addition to study the optical properties of DHI dimers and polymer. Paper V presents results on the photochemistry of DHICA oligomers and polymer. These results show the strength of the bottom up approach to facilitate the pigment study, and has allowed us to obtain a picture of the efficient photoprotection processes of the black eumelanin pigment. We also present the first preliminary results of excited state properties of synthetic eumelanin films. The films could be considered to be closer to the eumelanin pigment found in melanosomes of the skin than an aqueous solution of an eumelanin polymer, since films contain molecule/polymer agglomerates.

4.2.1- Paper IV: DHI dimers and polymer excited state properties

The poor solubility as well as the chemical disorder of eumelanin are main difficulties for the spectroscopic study of eumelanin. To overcome these difficulties, one method is to study the synthetic building blocks of the polymer and to synthetize oligomers and polymers out of the pure monomer. We can obtain homo-oligomers and polymer where the specific functionality of each unit in the whole melanin pigment can be determined. The aggregation and the precipitation in solution are more problematic. Herein we compare two solubilization methods. The DHI monomer and dimers, still soluble in buffer, are compared with monomer and dimers modified according to the two solubility methods.

The first solubilization method uses a buffer containing poly(vinyl alcohol) PVA at low concentration. The presence of PVA inhibits the interaction between the molecules and thus stops the aggregation. The second method is to add a sugar group at position 3 of the DHI molecule (for stucture see Figure 4−10). This method is referred to as a galactosyl-thio substitution since the substituent possesses a sulfur group as the linker. The resulting polymer is soluble in aqueous solution with optical properties similar to eumelanin. The samples from this

method will be referred to with the prefix gal, i.e. gal-DHI refers to the DHI monomer with a galactosyl-thio substitution at position 3. Polymerization with these two methods generates a similar dark soluble pigment containing free radical and similar optoelectronic character like the natural eumelanin.[110]

This study also gives us the opportunity to measure steady state optical properties and time-resolved fluorescence for DHI dimers and polymer for the first time.

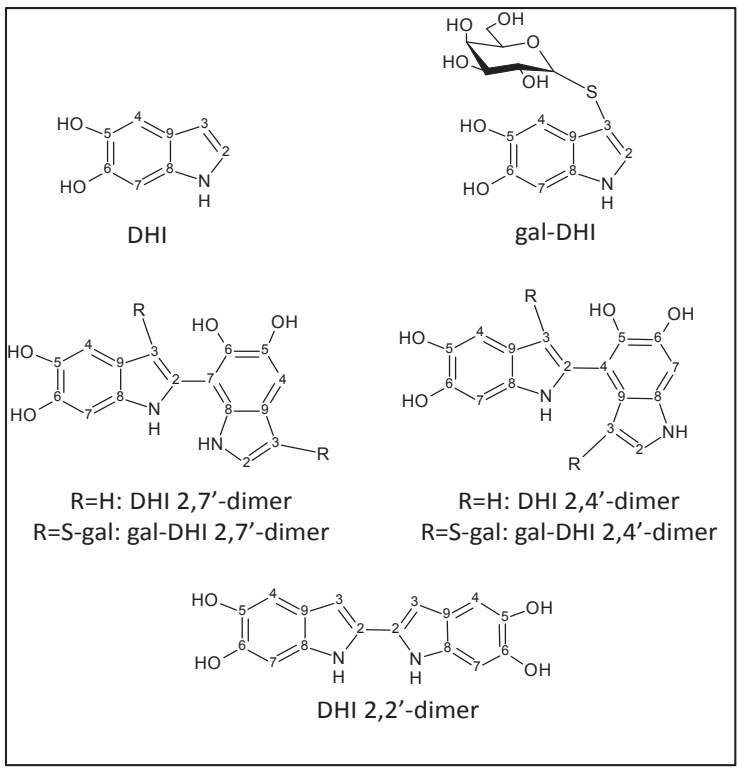

Figure 4-10: Structure of DHI and its derivatives, monomers and dimers, used for this study.

4.2.1.1- Steady state fluorescence measurements

Monomers

DHI in buffer and DHI in buffer/PVA present the same steady state characteristics two emission bands, a dominating one around 340 nm and a minor one around 380

nm. The gal-DHI in buffer is different although two emission bands are still distinguishable, but now the long-wavelength band is the dominating one; the whole spectrum is shifted to lower energy, Figure 4−11 (A).

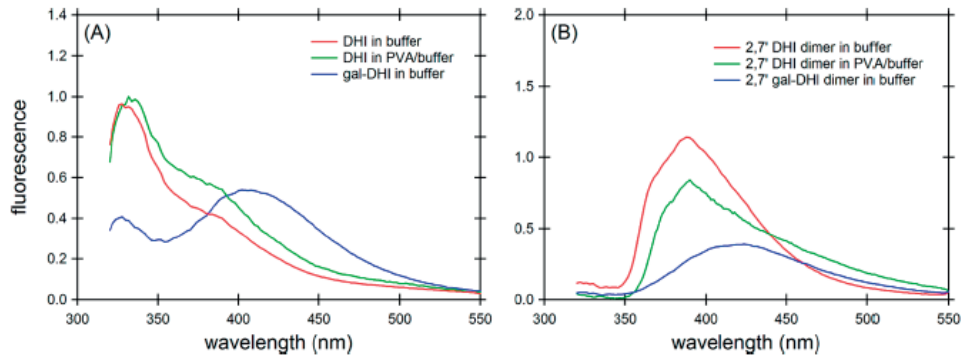

Figure 4-11: Steady state fluorescence spectra of (A) DHI and gal-DHI monomers and (B) DHI and gal-DHI 2,7' dimers in buffer and PVA/buffer.

Dimers

The global behavior of the dimers in buffer, buffer/PVA and the gal-dimers series are comparable. All show a very much reduced intensity of the high energy band present in the monomer spectrum and a red-shift of maxima compared to the DHI monomer, Figure 4−11 (B).

Polymers

The absorption properties of both the gal-DHI series and DHI polymers in buffer and buffer/PVA are not significantly different. The main differences are observed in their emission spectra. It should also be noticed that PVA has a non-negligible scattering contribution in the blue part of the spectrum. As mentioned above, a DHI-polymer is not soluble in buffer solution, but comparison of the fluorescence spectra of DHI-polymer in

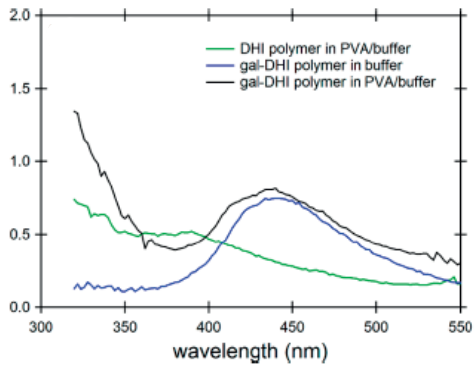

Figure 4-12: Steady state fluorescence spectra of DHI polymer in PVA/buffer, gal-DHI polymer in buffer and in PVA/buffer.

buffer/PVA and gal-DHI polymer shows that the spectra are similar and the emission intensity of the gal-DHI polymer is somewhat higher than for the polymer in buffer/PVA, Figure 4−12. In general the total emission intensity has decreased compared to the dimer emission. The sugar substitution, especially the presence of the sulfur group probably changes the electronic density of the indole core and the excited state dynamic is therefore altered compared to the DHI reference. Steady state optical measurements seem to demonstrate that PVA is a more appropriate method to solubilize DHI dimers and polymers, minimizing the spectral changes caused by the solubilization.

4.2.1.2- Time-resolved fluorescence measurements

The time-resolved fluorescence measurements suggest similar properties of DHI in buffer and DHI in buffer/PVA, Figure 4−13. As expected from the steady state spectra, the experimental data on the gal-series give different excited state dynamics. The sugar groups seems to reduce the interaction between the oligomer sub-units and give more monomer-like fluorescence kinetics Figure 4−13 (C). The obtained lifetimes for the fluorescence decays of DHI in buffer and for DHI in buffer/PVA are very similar, exhibiting a fast ~100 ps and slow ~1.7 ns decay, Figure 4−13 (A) and (B).

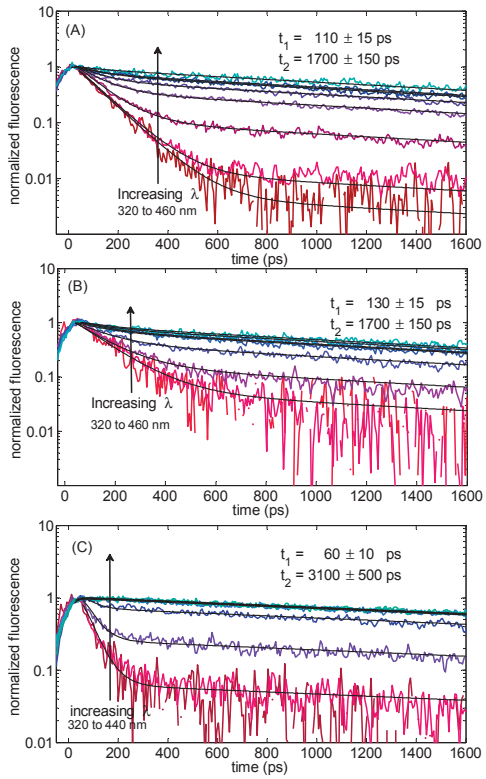

Figure 4-13: Time-resolved fluorescence decay kinetics upon 280 nm excitation of DHI monomer in (A) buffer, (B) DHI in PVA/buffer and (C) gal-DHI in buffer all with their fits.

DHI dimers show mono or bi-exponential fluorescence decay on the nanosecond timescale. The coupling of two DHI units together seems to efficiently reduce the rate of excited state decay. The three dimers in buffer solution have quite similar fluorescence decays; the 2,7' and the 2,2' (for structure refer to Figure 4−10) are fitted with a 960 ps and 1.3 ns single exponential lifetime, respectively,

Figure 4−14 (A), (B). The fluorescence decay of the 2,4' dimer required a low amplitude of a 150 ps lifetime in addition to the dominating 1.5 ns one, Figure 4−14 (D). Experiment on the same molecules but in buffer/PVA resulted in very similar lifetimes Figure 4−14 (C). As already mentioned above, the gal-dimers shows fluorescence kinetics more reminiscent of that for monomer DHI, Figure 4−14 (E) and (F). The 2,4' and 2,7' dimers present a short lifetime component on the blue side of their spectra on the order of 100 ps, and a longer one on the red-side of 760 and 620 ps. We interpret this difference as a result of reduced DHI-DHI interaction by the bulky sugar group, which make the dimers behave more as two non-interacting monomers.

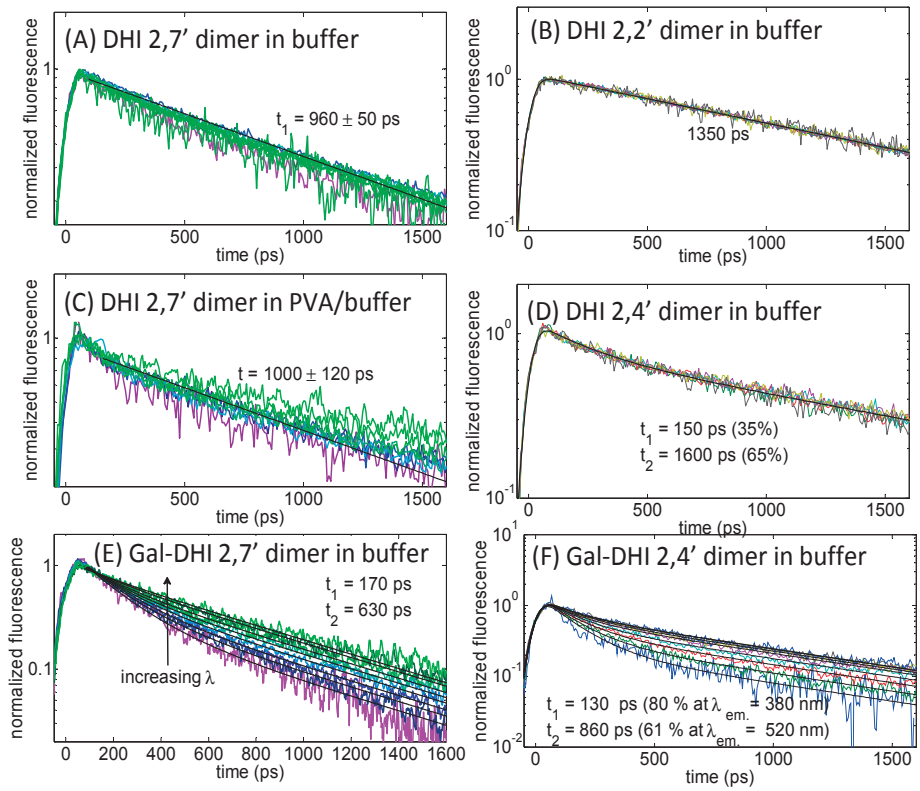

Figure 4-14: Time-resolved fluorescence traces of DHI dimers and derivatives in buffer or PVA/buffer upon 280 nm excitation, together with their fits. DHI 2,7'; 2,2' and 2,4' dimer in buffer are displayed in(A), (B) and (D) respectively. DHI 2,7' dimer in PVA/buffer is shown in (C) and the gal-DHI 2,7' and 2,4' dimers in buffer are presented in (E) and (F), respectively.

Both polymers in buffer/PVA and the gal-DHI polymer display a complex excited state decay from the ps to the ns timescale, Figure 4−15. While the polymer in buffer/PVA has the signature of a multiple species photochemical process with short lived (<100 ps) species in the high energy side of the spectrum and long lived component (1.6 to 3 ns) in the low energy region, the gal-DHI polymer exhibits a similar decay as its dimers, but with more of the ns component.

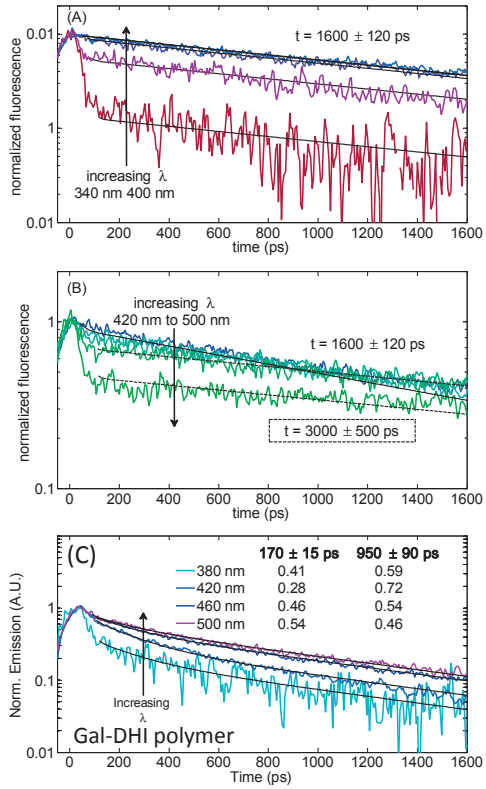

Figure 4-15: Time-resolved fluorescence traces DHI polymer in PVA/buffer (A-B) and gal-DHI polymer in buffer (C) upon 280 nm excitation, together with their fits. Graph (A) displays emission wavelengths from 340 nm to 400 nm, and graph (B) displays emission wavelength from 420 nm to 500 nm.

4.2.1.3- Conclusion Paper IV

Our measurements show without doubt that the best way to solubilize the polymer in aqueous solution is to use a PVA based solvent. The PVA only slightly affects the excited state dynamics. The galactosyl-thio substitution is an interesting approach, which does not seem to be optimal for the study of the unperturbed excited state, but this method can give some insight into the excited state dynamics by influencing the electron cloud. In addition this paper is the first one to reveal the optical properties of the three main dimers arising from DHI and the homopolymer. It is important to note that fast relaxation observed for DHI seems to slow down by increasing the length of the chain. This is consistent with the belief that DHI-based pigments have less photoprotective properties than DHICA – the long lived excited state species could be the explanation.

4.2.2- Paper V: DHICA oligomers - efficient photoprotection against UV light

As described above DHICA is an essential component of the eumelanin polymer. In vitro synthesis is found to yield larger proportions of DHI-based pigment than pigments having DHICA as building blocks, but it was observed that in vivo, DHICA accounts for at least 50 % of the polymer composition.[20]

Here we present the photochemical processes following UV-absorption by DHICA oligomers and polymer. Two differently connected dimers, a trimer and the polymer were studied using streak camera and fluorescence up-conversion time-resolved fluorescence. With the same methods applied for the DHICA monomer and the DHI units, the samples were studied under acidic and neutral condition in order to control the ground state population. Methanol was also used to observe the solvent effect on the dissipation mechanism.

Steady state absorption maxima of the DHICA oligomers present a red-shift with chain elongation. As for the monomer a red shift is observed in acidic condition compared to the neutral one. The absorption bands of the oligomers show approximately the same width as the monomer. The covalent bond between the monomer units suggest free rotation between the monomer units, resulting in a large range of configurations. The polymer absorption spectrum is similar to the dimers, but a featureless red shoulder resembling the absorption spectrum of eumelanin is present.

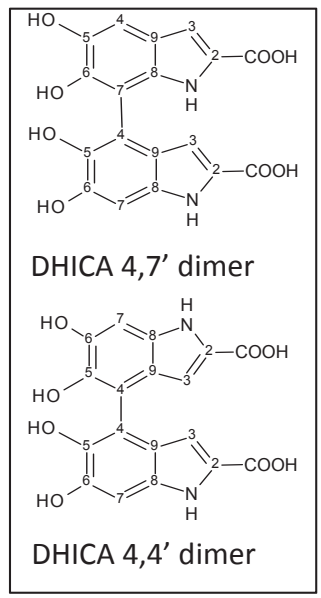

Figure 4-16: Structure of DHICA dimers used for this study.

The first striking observation from the time-resolved fluorescence measurements is the ultrafast decay obtained at neutral condition (pH 7), Figure 4–17 (A). While the monomer presents a long emission lifetime on the nanosecond timescale, for the dimers almost all the emission has decayed after a picosecond. The measured lifetime is 300 fs –1000 fold faster than the monomer decay at pH 7. The polymer at pH 7 also presents a very fast decay of 190 fs. Measurements in D_2O do not show a significant KIE. The second main observation is that the 4,4' and 4.7' dimers have very similar fluorescence decays.

Stuctures of the dimers is shown in Figure 4−16. Obviously, the excited state decay is not sensitive to the exact mode of monomer-monomer coupling. Measurements in acidic solution also show a faster decay rate for the dimers than for the monomer, 190 fs for the dimers as compared to 300 fs for the monomer, Figure 4−17 (B).

The experiments in neutral condition show that covalent bonding opens up a new energy dissipation channel. Though the energy dissipation time is much faster than for the monomer, we conclude that ESPT seems to be the main mechanism of excited state decay. Before we could assign the ultrafast excited state decay of DHICA dimers, oligomers and polymer to an ESPT process, two other relaxation mechanisms had to be considered, conformational dynamics and exciton dynamics. Experiments in different solvents rule out the conformational dynamics mechanism. Conformational changes are expected to be highly dependent on solvent viscosity, the more viscous the solvent the slower the excited state decay. We do not observe this, on contrary we observed a much slower decay rate in methanol (~10 ps) compared to aqueous solution (~200 fs). In the case of exciton dynamics, the absorption spectra of the dimers compared to the monomer do not support this mechanism as being responsible of the fast decay observed in the fluorescence measurements. If strong exciton interactions, leading to ultrafast exciton relaxation, would be present, the absorption spectra should present a blue-shift instead of the observed red-shifts, due to the sandwich configuration of the transition dipole moments of the monomer units. In addition the flexibility of the bond between the two units would cause a broadening of the absorption band, which is not observed.

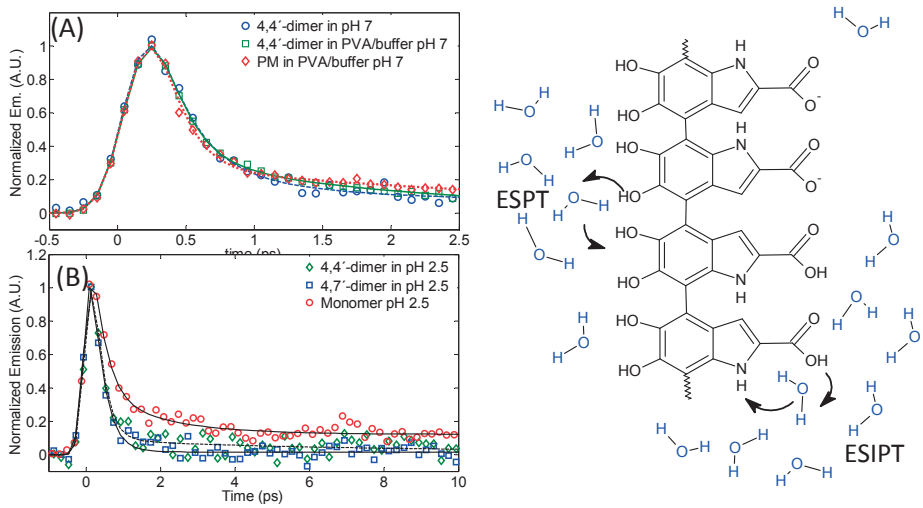

Figure 4-17: Left panel, graph (A) shows the emission decays of the DHICA 4,4' dimer in pH 7, in PVA/pH 7 and the polymer in PVA/pH7 measured at 380 nm upon 267 nm excitation. Graph (B) shows the emission decays of DHICA monomer and 4,4' and 4,7' dimers in pH 2.5 buffer solution, mesurured at 380 nm upon 267 nm excitation. Right panel, DHICA polymer relaxation mechanism via ESIPT and ESPT after UV irradiation.

All this led us to conclude that ESPT is the main mechanism responsible for the ultrafast sub-ps excited state decay in dimers, oligomers and polymer of DHICA. In acidic condition we believed that as for the monomer, dimers have an ESIPT from the COOH to the NH group. This is supported by the presence of a red shifted emission band above 420 nm (like for the monomer), with a lifetime of ~140 ps, Figure 4−18. We attributed this band to the zwitterion photoproduct of the ESIPT, similar to the one observed in the relaxation mechanism of the DHICA monomer at pH 2.5. At pH 7 we demonstrated that the monomer undergoes a slow ESPT from the OH groups to the solvent, which lead to the double anion photoproduct. The photoproduct was shown to have a relaxation time of 2.4 ns. For the dimers and upward oligomers, we believe that ESPT is also the mechanism of excited state decay, but the ESPT is very much accelerated as

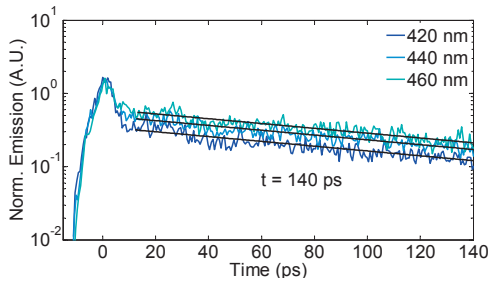

Figure 4-18: Time-resolved fluorescence traces of DHICA at pH 2.5 recorded between 20 and 460 nm upon 280 nm excitation. Fits are shown in black and result in a 140 ps lifetime.

compared to the monomer. We suggest that the higher ESPT rate for the dimers and higher oligomers is a result of a proton cage formed by the hydroxyl groups of the surrounding DHICA units and the solvent, similar to what was suggested for substituted 2-naphthols by Tolbert et al.[94] Another explanation could be the formation of a proton wire as observed for the green fluorescent protein.[111,112] Both models demonstrated that a network of pre-existing hydrogen bonds can give rise to fast and very efficient proton transfer.

Our results did not show any red-shifted fluorescence that could be attributed to the proton transfer photoproduct. This leads to two possible conclusions: either the photoproduct is formed in the ground state, or decays very rapidly via internal conversion. The proposed proton cage or wire would lead to an efficient solvation of the proton (and therefore fast ESPT), as well as an efficient recombination of the ground state species. Fluorescence steady state measurements at basic pH of the dimers, where the carboxyl and the hydroxyl groups are deprotonated, present weak fluorescence signal not observed at neutral condition. This is an indication of the hydroxyl group participation in the excited state relaxation. The mechanism proposed for the dimer is also valid for the polymer since the measured dynamics is very similar, only slightly more rapid. The experiments demonstrate the importance of the solvent in the dissipation process, since we see that in methanol the excited state decay is slowed down to 10 ps. This is probably due to the poorer proton accepting capacity of methanol compared to water.

4.2.4.1- Conclusion Paper V

Now taking all observations together, we conclude that two types of excited state proton transfer are active in eumelanin, causing efficient UV-dissipation. ESIPT from COOH to NH assisted by water molecules, and ESPT from the hydroxyl groups with the help of a proton accepting cage formed by OH groups from other DHICA subunits and water molecules. This results in an ultrafast ESIPT + ESPT with a rate of $(200\ fs)^{-1}$. Compared to the DHI homopolymer, the DHICA polymer is much more efficient to dissipate the harmful energy of UV-light.

4.2.3- DHI and DHICA thin films

In the melanosome melanins exist in the form of an aggregate, close to the solid state. In order to get some insight into the properties of solid state melanin and its relation to solution structure, we have performed preliminary experiments on thin

film samples of DHI and DHICA monomers and polymers deposed on a quartz substrate. In addition, the study of films overcomes the solubility problem and makes it easy to study different derivatives. The samples contain a low amount of water and the molecules are closely stacked. DHI and DHICA monomers deposited on a quartz substrate have emission decays much faster than in solution; after 100 ps there is no longer any emission detectable. The DHI films have a response faster than 3 ps and we have not been able to fully resolve the emission decay from either the monomer or the polymer with the streak camera. On the other hand, for DHICA the fluorescence decays are somewhat slower and can be resolved with the streak camera. For both monomer and polymer samples the fluorescence decays are emission wavelength dependent. For the DHICA monomer, the fluorescence was measured between 380 nm to 580 nm and a short, < 3 ps lifetime was observed on the blue side of the emission spectrum and a longer, 42 ps one on the red side, Figure 4−19. For the polymer DHICA approximately the same lifetimes were obtained, but the intensity of the red emission is lower compared to the monomer.

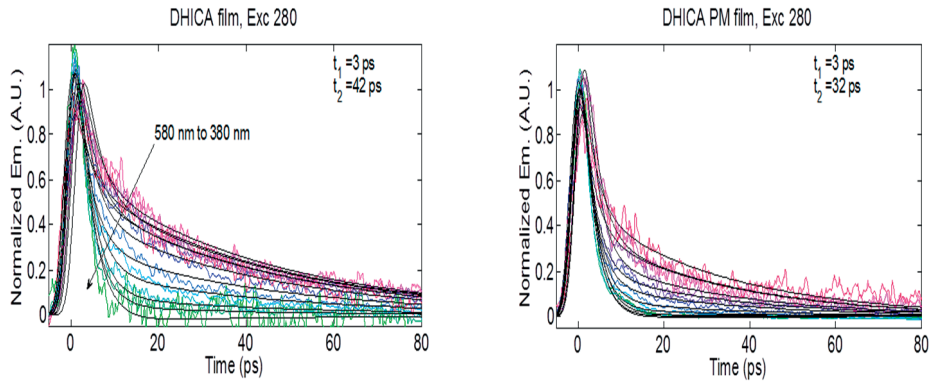

Figure 4-19: Time-resolved fluorescence traces of DHICA film, monomer (left panel) and polymer (right panel) upon 280 nm excitation measured bewteen 380 nm and 580 nm (purple to green), together with their exponential fits (black). Two lifetimes were obtained 3 ps and 42 ps for the monomer and 3 ps and 32 ps for the polymer.

We also performed measurements on films of three derivatives of DHICA with either of the proton donating groups substituted with methyl groups inhibiting proton transfer to an aqueous solvent; ICA where the hydroxyl groups are missing, the methyl ester of DHICA, where the hydrogen of the carboxyl group is replaced by a methyl and finally the per-methylated ester, where the two hydrogens of the hydroxyl groups as well as the hydrogen of the carboxyl are replaced by methyl

groups. The time-resolved fluorescence measurements performed on these three films exhibit complex non-exponential emission decays. Similarly to DHI and DHICA monomers and polymers, fast few tens of picoseconds decays are observed on the blue side of the fluorescence spectrum and longer hundreds of picoseconds decay on the red side. Thus, although the proton transfer capability of these substituted DHICA monomers have been reduced or eliminated, fast fluorescence decays are observed in the solid state. This, along with the very short lifetimes of the DHI and DHICA monomer and polymer films suggests that in the solid state, which may mimic the conditions in the melanosome, there are interactions and relaxation pathways not present in the solution phase. What these processes are is not clear at the moment and are topics of future investigations.

4.2.4- Polymer Conclusion

The spectroscopic study of the two solubilizing methods, PVA and gal-substitution, allowed us to find a method to make eumelanin building blocks with poor solubility, soluble in aqueous solution, without too much affecting the dynamics of the samples. The solvent mixture buffer/PVA allowed us to study oligomers and polymers in solution without strong influence on the photochemistry of the sample. We have shown that DHI and DHICA in solution and in film have different properties. DHICA oligomers and polymer efficiently dissipate UV excited state energy by ESPT/ESIPT assisted by water molecules in solution. In the solid state, DHICA monomers and polymer also exhibit efficient excited state deactivation, but the mechanisms remain to be established. In solution DHI oligomers and polymers present rather long excited state lifetimes which makes them more likely to be involved in formation of reactive species and harmful reactions, which could eventually lead to tissue damage. DHI in the solid state, dissipates excited state energy even more efficiently than DHICA, but also here the mechanisms remain to be established.

5- Conclusion and Future Work

By a bottom-up approach we have been able to differentiate the properties of the two eumelanin building blocks DHI and DHICA and to understand the role of the aggregation state for their photochemical properties. DHICA in solution has a very efficient excited state deactivation, especially in its polymer form. Efficient Excited State Proton Transfer assisted by water molecules, from either the carboxyl group to the nitrogen, or from the hydroxyl groups to the solvent allows relaxation of the molecules to their ground state in a few picoseconds. The double ESPT/ESIPT channels for excited state energy dissipation results in a robust mechanism for efficient photoprotection.

For DHI in solution, the excited state relaxation pathways are similar to those of anionic DHICA, controlled by ESPT from the hydroxyl groups. The polymer, however, shows opposite properties – the DHI homo-polymer has a much longer nanosecond lifetime, possibly leading to phototoxic channels that could lead to melanoma. When the building blocks are deposited as a thin solid film, forming tight aggregation, this difference between DHI and DHICA essentially disappears. Both pigments exhibit short picosecond timescale excited state lifetimes; thin films of DHI in fact have even shorter fluorescence lifetimes than films of DHICA. The fact that DHI and DHICA oligomers and polymers both in solution and the solid state, jointly provide very efficient excited state deactivation, could be Nature's strategy to "by all means" achieve efficient photoprotection against the harmful effects of UV-light.

We have made important progress in the understanding of photochemical mechanisms of eumelanin and its building blocks in solution, and we have identified excited state proton transfer as important mechanisms for excited state energy dissipation. However, in melanosomes the aggregation state and pigment environment may be closer to the solid state than solution. Therefore, study of eumelanin in the solid state is an important future direction of melanin research. Our first preliminary results shows that additional processes come into play in comparison to the solution case. Extending these studies to e.g. other techniques

and modified building blocks will hopefully provide more insights into the relaxation mechanisms present in the solid state. Finally, the calculations performed on ICA, DHI and $DHICA^-$, show that this is a valuable complement to the experimental work that can provide additional insight into relaxation mechanisms. Future calculations will hopefully help to shed light into the origin of the very fast excited state decays of DHICA oligomers and the solid state samples.

References

1. Ito, S.; Wakamatsu, K. Human hair melanins: what we have learned and have not learned from mouse coat color pigmentation. Pigment Cell & Melanoma Research 2011, 24 (1), 63-74.
2. Prota G . Melanins and Melanogenesis; Academic Press: San Diego, CA. Melanins and melanogenesis (Academic Press, San Diego) . 1992.
3. Abdel-Mallek, Z. A.; Knittel, J.; Kadekaro, A. L.; Swope, V. B.; Starner, R. The melanocortin 1 receptor and the UV response of human melanocytes - A shift in paradigm. Photochemistry and Photobiology 2008, 84 (2), 501-508.
4. Ito, S. High-Performance Liquid-Chromatography (Hplc) Analysis of Eumelanin and Pheomelanin in Melanogenesis Control. Journal of Investigative Dermatology 1993, 100 (2), S166-S171.
5. Kollias, N.; Sayre, R. M.; Zeise, L.; Chedekel, M. R. Photoprotection by Melanin. Journal of Photochemistry and Photobiology B-Biology 1991, 9 (2), 135-160.
6. Ito, S.; Wakamatsu, K. Chemistry of mixed melanogenesis - Pivotal roles of dopaquinone. Photochemistry and Photobiology 2008, 84 (3), 582-592.
7. Tran, M. L.; Powell, B. J.; Meredith, P. Chemical and structural disorder in eumelanins: A possible explanation for broadband absorbance. Biophysical Journal 2006, 90 (3), 743-752.
8. Chedekel, M. R.; Smith, S. K.; Post, P. W.; Pokora, A.; Vessell, D. L. Photodestruction of Pheomelanin - Role of Oxygen. Proceedings of the National Academy of Sciences of the United States of America 1978, 75 (11), 5395-5399.
9. Chedekel, M. R.; Land, E. J.; Sinclair, R. S.; Tait, D.; Truscott, T. G. Photochemistry of 4-Hydroxybenzothiazole - A Model for Pheomelanin Photodegradation. Journal of the American Chemical Society 1980, 102 (21), 6587-6590.
10. De Leeuw, S. M.; Smit, N. P. M.; Van Veldhoven, M.; Pennings, E. M.; Pavel, S.; Simons, J. W. I. M.; Schothorst, A. A. Melanin content of cultured human melanocytes and UV-induced cytotoxicity. Journal of Photochemistry and Photobiology B-Biology 2001, 61 (3), 106-113.
11. Samokhvalov, A.; Hong, L.; Liu, Y.; Garguilo, J.; Nemanich, R. J.; Edwards, G. S.; Simon, J. D. Oxidation potentials of human eumelanosomes and plheomelanosomes. Photochemistry and Photobiology 2005, 81 (1), 145-148.
12. Takeuchi, S.; Zhang, W. G.; Wakamatsu, K.; Ito, S.; Hearing, V. J.; Kraemer, K. H.; Brash, D. E. Melanin acts as a cause an atypical potent UVB photosensitizer to mode of cell death in murine skin. Proceedings of the National Academy of Sciences of the United States of America 2004, 101 (42), 15076-15081.

13. Charkoudian, L. K.; Franz, K. J. Fe(III)-coordination properties of neuromelanin components: 5,6-dihydroxyindole and 5,6-dihydroxyindole-2-carboxylic acid. Inorganic Chemistry 2006, 45 (9), 3657-3664.

14. Gotz, M. E.; Double, K.; Gerlach, M.; Youdim, M. B. H.; Riederer, P. The relevance of iron in the pathogenesis of Parkinson's disease. Redox-Active Metals in Neurological Disorders 2004, 1012, 193-208.

15. Liu, Y.; Simon, J. D. Metal-ion interactions and the structural organization of Sepia eumelanin. Pigment Cell Research 2005, 18 (1), 42-48.

16. Simon, J. D.; Ito, S. The chemical structure of melanin - Reply. Pigment Cell Research 2004, 17 (4), 423-424.

17. Napolitano, A.; Corradini, M. G.; Prota, G. A Reinvestigation of the Structure of Melanochrome. Tetrahedron Letters 1985, 26 (23), 2805-2808.

18. Pezzella, A.; Napolitano, A.; dIschia, M.; Prota, G. Oxidative polymerisation of 5,6-dihydroxyindole-2-carboxylic acid to melanin: A new insight. Tetrahedron 1996, 52 (23), 7913-7920.

19. Felix, C. C.; Hyde, J. S.; Sarna, T.; Sealy, R. C. Melanin Photoreactions in Aerated Media - Electron-Spin Resonance Evidence for Production of Superoxide and Hydrogen-Peroxide. Biochemical and Biophysical Research Communications 1978, 84 (2), 335-341.

20. Meredith, P.; Sarna, T. The physical and chemical properties of eumelanin. Pigment Cell Research 2006, 19 (6), 572-594.

21. Nofsinger, J. B.; Simon, J. D. Radiative relaxation of Sepia eumelanin is affected by aggregation. Photochemistry and Photobiology 2001, 74 (1), 31-37.

22. Stark, K. B.; Gallas, J. M.; Zajac, G. W.; Eisner, M.; Golab, J. T. Spectroscopic study and simulation from recent structural models for eumelanin: II. Oligomers. Journal of Physical Chemistry B 2003, 107 (41), 11558-11562.

23. Stark, K. B.; Gallas, J. M.; Zajac, G. W.; Eisner, M.; Golab, J. T. Spectroscopic study and simulation from recent structural models for eumelanin: I. Monomer, dimers. Journal of Physical Chemistry B 2003, 107 (13), 3061-3067.

24. Stark, K. B.; Gallas, J. M.; Zajac, G. W.; Golab, J. T.; Gidanian, S.; McIntire, T.; Farmer, P. J. Effect of stacking and redox state on optical absorption spectra of melanins-comparison of theoretical and experimental results. Journal of Physical Chemistry B 2005, 109 (5), 1970-1977.

25. Pezzella, A.; Crescenzi, O.; Panzella, L.; Napolitano, A.; Land, E. J.; Barone, V.; d'Ischia, M. Free Radical Coupling of o-Semiquinones Uncovered. Journal of the American Chemical Society 2013, 135 (32), 12142-12149.

26. Bertazzo, A.; Costa, C.; Allegri, G.; Seraglia, R.; Traldi, P. Biosynthesis of Melanin from Dopamine - An Investigation of Early Oligomerization Products. Rapid Communications in Mass Spectrometry 1995, 9 (8), 634-640.

27. Bertazzo, A.; Costa, C. V. L.; Allegri, G.; Schiavolin, M.; Favretto, D.; Traldi, P. Enzymatic oligomerization of tyrosine by tyrosinase and peroxidase studied by matrix-assisted laser desorption/ionization mass spectrometry. Rapid Communications in Mass Spectrometry 1999, 13 (6), 542-547.

28. Costa, C.; Bertazzo, A.; Allegri, G.; Toffano, G.; Curcuruto, O.; Traldi, P. Melanin Biosynthesis from Dopamine .2. A Mass-Spectrometric and Collisional Spectroscopic Investigation. Pigment Cell Research 1992, 5 (3), 122-131.

29. Kroesche, C.; Peter, M. G. Detection of melanochromes by MALDI-TOF mass spectrometry. Tetrahedron 1996, 52 (11), 3947-3952.

30. Napolitano, A.; Pezzella, A.; Prota, G.; Seraglia, R.; Traldi, P. Structural analysis of synthetic melanins from 5,6-dihydroxyindole by matrix-assisted laser desorption ionization mass spectrometry. Rapid Communications in Mass Spectrometry 1996, 10 (4), 468-472.

31. Pezzella, A.; Napolitano, A.; dIschia, M.; Prota, G.; Seraglia, R.; Traldi, P. Identification of partially degraded oligomers of 5,6-dihydroxyindole-2-carboxylic acid in Sepia melanin by matrix-assisted laser desorption/ionization mass spectrometry. Rapid Communications in Mass Spectrometry 1997, 11 (4), 368-372.

32. Lindgren, J.; Uvdal, P.; Sjovall, P.; Nilsson, D. E.; Engdahl, A.; Schultz, B. P.; Thiel, V. Molecular preservation of the pigment melanin in fossil melanosomes. Nature Communications 2012, 3.

33. Meredith, P.; Riesz, J. Radiative relaxation quantum yields for synthetic eumelanin. Photochemistry and Photobiology 2004, 79 (2), 211-216.

34. Riesz, J.; Sarna, T.; Meredith, P. Radiative relaxation in synthetic pheomelanin. Journal of Physical Chemistry B 2006, 110 (28), 13985-13990.

35. Nighswander-Rempel, S. P. Quantitative fluorescence spectra and quantum yield map of synthetic pheomelanin. Biopolymers 2006, 82 (6), 631-637.

36. Nighswander-Rempel, S. P.; Riesz, J.; Gilmore, J.; Meredith, P. A quantum yield map for synthetic eumelanin. Journal of Chemical Physics 2005, 123 (19).

37. Riesz, J.; Gilmore, J.; Meredith, P. Quantitative scattering of melanin solutions. Biophysical Journal 2006, 90 (11), 4137-4144.

38. Forest, S. E.; Lam, W. C.; Millar, D. P.; Nofsinger, J. B.; Simon, J. D. A model for the activated energy transfer within eumelanin aggregates. Journal of Physical Chemistry B 2000, 104 (4), 811-814.

39. Teuchner, K.; Freyer, W.; Leupold, D.; Volkmer, A.; Birch, D. J. S.; Altmeyer, P.; Stucker, M.; Hoffmann, K. Femtosecond two-photon excited fluorescence of melanin. Photochemistry and Photobiology 1999, 70 (2), 146-151.

40. Teuchner, K.; Ehlert, J.; Freyer, W.; Leupold, D.; Altmeyer, P.; Stucker, M.; Hoffmann, K. Fluorescence studies of melanin by stepwise two-photon femtosecond laser excitation. Journal of Fluorescence 2000, 10 (3), 275-281.

41. Ye, T.; Simon, J. D. Comparison of the ultrafast absorption dynamics of eumelanin and pheomelanin. Journal of Physical Chemistry B 2003, 107 (40), 11240-11244.

42. Forest, S. E.; Simon, J. D. Wavelength-dependent photoacoustic calorimetry study of melanin. Photochemistry and Photobiology 1998, 68 (3), 296-298.

43. Nofsinger, J. B.; Ye, T.; Simon, J. D. Ultrafast nonradiative relaxation dynamics of eumelanin. Journal of Physical Chemistry B 2001, 105 (14), 2864-2866.

44. Edge, R.; d'Ischia, M.; Land, E. J.; Napolitano, A.; Navaratnam, S.; Panzella, L.; Pezzella, A.; Ramsden, C. A.; Riley, P. A. Dopaquinone redox exchange with

dihydroxyindole and dihydroxyindole carboxylic acid. Pigment Cell Research 2006, 19 (5), 443-450.

45. Pezzella, A.; Iadonisi, A.; Valerio, S.; Panzella, L.; Napolitano, A.; Adinolfi, M.; d'Ischia, M. Disentangling Eumelanin "Black Chromophore": Visible Absorption Changes As Signatures of Oxidation State- and Aggregation-Dependent Dynamic Interactions in a Model Water-Soluble 5,6-Dihydroxyindole Polymer. Journal of the American Chemical Society 2009, 131 (42), 15270-15275.
46. Wakamatsu, K.; Ito, S. Preparation of Eumelanin-Related Metabolites 5,6-Dihydroxyindole, 5,6-Dihydroxyindole-2-Carboxylic Acid, and Their O-Methyl Derivatives. Analytical Biochemistry 1988, 170 (2), 335-340.
47. d'Ischia, M.; Napolitano, A.; Pezzella, A.; Land, E. J.; Ramsden, C. A.; Riley, P. A. 5,6-dihydroxyrindoles and Indole-5,6-diones. Advances in Heterocyclic Chemistry, Vol 89 2005, 89, 1-63.
48. Pezzella, A.; Vogna, D.; Prota, G. Synthesis of optically active tetrameric melanin intermediates by oxidation of the melanogenic precursor 5,6-dihydroxyindole-2-carboxylic acid under biomimetic conditions. Tetrahedron-Asymmetry 2003, 14 (9), 1133-1140.
49. Capelli, L.; Manini, P.; Pezzella, A.; Napolitano, A.; d'Ischia, M. Efficient Synthesis of 5,6-Dihydroxyindole Dimers, Key Eumelanin Building Blocks, by a Unified o-Ethynylaniline-Based Strategy for the Construction of 2-Linked Biindolyl Scaffolds. Journal of Organic Chemistry 2009, 74 (18), 7191-7194.
50. Nighswander-Rempel, S. P. Quantum yield calculations for strongly absorbing chromophores. Journal of Fluorescence 2006, 16 (4), 483-485.
51. Gustavsson, T.; Cassara, L.; Gulbinas, V.; Gurzadyan, G.; Mialocq, J. C.; Pommeret, S.; Sorgius, M.; van der Meulen, P. Femtosecond spectroscopic study of relaxation processes of three amino-substituted coumarin dyes in methanol and dimethyl sulfoxide. Journal of Physical Chemistry A 1998, 102 (23), 4229-4245.
52. Caldin, E. F. and Gold, V., Chapmann and Hall, London. Proton-transfer reactions. 1975.
53. Douhal, A.; Kim, S. K.; Zewail, A. H. Femtosecond Molecular-Dynamics of Tautomerization in Model Base-Pairs. Nature 1995, 378 (6554), 260-263.
54. Sakota, K.; Sekiya, H. Excited-state double-proton transfer in the 7-azaindole dimer in the gas phase. 2. Cooperative nature of double-proton transfer revealed by H/D kinetic isotopic effects. Journal of Physical Chemistry A 2005, 109 (12), 2722-2727.
55. Fuke, K.; Ishikawa, H. Dynamics of proton transfer reactions of model base pairs in the ground and excited states: Revisited. Chemical Physics Letters 2015, 623, 117-129.
56. Wu, Y. S.; Huang, H. C.; Shen, J. Y.; Tseng, H. W.; Ho, J. W.; Chen, Y. H.; Chou, P. T. Water-Catalyzed Excited-State Proton-Transfer Reactions in 7-Azaindole and Its Analogues. Journal of Physical Chemistry B 2015, 119 (6), 2302-2309.
57. Weller, A. Quantitative Untersuchungen der Fluoreszenzumwandlung Bei Naphtholen. Zeitschrift fur Elektrochemie 1952, 56 (7), 662-668.
58. Hynes, J. T.; Tran-Thi, T. H.; Granucci, G. Intermolecular photochemical proton transfer in solution: new insights and perspectives. Journal of Photochemistry and Photobiology A-Chemistry 2002, 154 (1), 3-11.

59. Domcke, W.; Sobolewski, A. L. Chemistry - Unraveling the molecular mechanisms of photoacidity. Science 2003, 302 (5651), 1693-1694.

60. Tolbert, L. M.; Solntsev, K. M. Excited-state proton transfer: From constrained systems to "super" photoacids to superfast proton transfer. Accounts of Chemical Research 2002, 35 (1), 19-27.

61. Agmon, N. Elementary steps in excited-state proton transfer. Journal of Physical Chemistry A 2005, 109 (1), 13-35.

62. Sobolewski, A. L.; Domcke, W.; Dedonder-Lardeux, C.; Jouvet, C. Excited-state hydrogen detachment and hydrogen transfer driven by repulsive (1)pi sigma* states: A new paradigm for nonradiative decay in aromatic biomolecules. Physical Chemistry Chemical Physics 2002, 4 (7), 1093-1100.

63. Gregoire, G.; Dedonder-Lardeux, C.; Jouvet, C.; Martrenchard, S.; Peremans, A.; Solgadi, D. Picosecond hydrogen transfer in the phenol-(NH3)(n=1-3) excited state. Journal of Physical Chemistry A 2000, 104 (40), 9087-9090.

64. Ishiuchi, S.; Saeki, M.; Sakai, M.; Fujii, M. Infrared dip spectra of photochemical reaction products in a phenol/ammonia cluster: examination of intracluster hydrogen transfer. Chemical Physics Letters 2000, 322 (1-2), 27-32.

65. Tolbert, L. M.; Harvey, L. C.; Lum, R. C. Excited-State Proton-Transfer from Hydroxyalkylnaphthols. Journal of Physical Chemistry 1993, 97 (50), 13335-13340.

66. Cohen, B.; Huppert, D. Evidence for a continuous transition from nonadiabatic to adiabatic proton transfer dynamics in protic liquids. Journal of Physical Chemistry A 2001, 105 (13), 2980-2988.

67. Bell, R. P. The Proton in Chemistry; Ithaca, 1973.

68. Bell, R. P. The Tunnel Effect in Chemistry; London, 1980.

69. Erez, Y.; Huppert, D. Excited-State Intermolecular Proton Transfer of the Firefly's Chromophore D-Luciferin. Journal of Physical Chemistry A 2010, 114 (31), 8075-8082.

70. Robinson, G. W.; Thistlethwaite, P. J.; Lee, J. Molecular Aspects of Ionic Hydration Reactions. Journal of Physical Chemistry 1986, 90 (18), 4224-4233.

71. Pines, E.; Fleming, G. R. Proton-Transfer in Mixed Water Organic-Solvent Solutions - Correlation Between Rate, Equilibrium-Constant, and the Proton Free-Energy of Transfer. Journal of Physical Chemistry 1991, 95 (25), 10448-10457.

72. Agmon, N.; Huppert, D.; Masad, A.; Pines, E. Excited-State Proton-Transfer to Methanol Water Mixtures. Journal of Physical Chemistry 1991, 95 (25), 10407-10413.

73. Agmon, N. Correction. Journal of Physical Chemistry 1992, 96 (4), 2020.

74. Borgis, D.; Hynes, J. T. Curve crossing formulation for proton transfer reactions in solution. Journal of Physical Chemistry 1996, 100 (4), 1118-1128.

75. Cohen, B.; Segal, J.; Huppert, D. Proton transfer from photoacid to solvent. Journal of Physical Chemistry A 2002, 106 (32), 7462-7467.

76. Solntsev, K. M.; Huppert, D.; Agmon, N.; Tolbert, L. M. Photochemistry of "super" photoacids. 2. Excited-state proton transfer in methanol/water mixtures. Journal of Physical Chemistry A 2000, 104 (19), 4658-4669.

77. Leiderman, P.; Genosar, L.; Huppert, D. Excited-state proton transfer: Indication of three steps in the dissociation and recombination process. Journal of Physical Chemistry A 2005, 109 (27), 5965-5977.

78. Tran-Thi, T. H.; Gustavsson, T.; Prayer, C.; Pommeret, S.; Hynes, J. T. Primary ultrafast events preceding the photoinduced proton transfer from pyranine to water. Chemical Physics Letters 2000, 329 (5-6), 421-430.

79. Formosinho, S. J.; Arnaut, L. G. Excited-State Proton-Transfer Reactions .2. Intramolecular Reactions. Journal of Photochemistry and Photobiology A-Chemistry 1993, 75 (1), 21-48.

80. Douhal, A.; Lahmani, F.; Zewail, A. H. Proton-transfer reaction dynamics. Chemical Physics 1996, 207 (2-3), 477-498.

81. Douhal, A.; Lahmani, F.; Zehnackerrentien, A.; Amatguerri, F. Excited-State Proton (Or Hydrogen-Atom) Transfer in Jet-Cooled 2-(2'-Hydroxyphenyl)-5-Phenyloxazole. Journal of Physical Chemistry 1994, 98 (47), 12198-12205.

82. Weller, A. Fast Reactions of Excited Molecules. Progress in Reaction Kinetics and Mechanism 1961, 1, 187-&.

83. Laws, W. R.; Brand, L. Analysis of 2-State Excited-State Reactions - Fluorescence Decay of 2-Naphthol. Journal of Physical Chemistry 1979, 83 (7), 795-802.

84. Webb, S. P.; Philips, L. A.; Yeh, S. W.; Tolbert, L. M.; Clark, J. H. Picosecond Kinetics of the Excited-State, Proton-Transfer Reaction of 1-Naphthol in Water. Journal of Physical Chemistry 1986, 90 (21), 5154-5164.

85. Kosower, E. M.; Huppert, D. Excited-State Electron and Proton Transfers. Annual Review of Physical Chemistry 1986, 37, 127-156.

86. Agmon, N. Diffusion with Back Reaction. Journal of Chemical Physics 1984, 81 (6), 2811-2817.

87. Agmon, N.; Pines, E.; Huppert, D. Geminate Recombination in Proton-Transfer Reactions .2. Comparison of Diffusional and Kinetic Schemes. Journal of Chemical Physics 1988, 88 (9), 5631-5638.

88. Pines, E.; Huppert, D.; Agmon, N. Geminate Recombination in Excited-State Proton-Transfer Reactions - Numerical-Solution of the Debye-Smoluchowski Equation with Backreaction and Comparison with Experimental Results. Journal of Chemical Physics 1988, 88 (9), 5620-5630.

89. Lumry, R.; Hershberger, M. Status of Indole Photochemistry with Special Reference to Biological Applications. Photochemistry and Photobiology 1978, 27 (6), 819-840.

90. Medina, F.; Poyato, J. M. L.; Pardo, A.; Rodriguez, J. G. Photophysical Study of Some Indole-Derivatives. Journal of Photochemistry and Photobiology A-Chemistry 1992, 67 (3), 301-310.

91. Petrich, J. W.; Chang, M. C.; Mcdonald, D. B.; Fleming, G. R. On the Origin of Non-Exponential Fluorescence Decay in Tryptophan and Its Derivatives. Journal of the American Chemical Society 1983, 105 (12), 3824-3832.

92. Robbins, R. J.; Fleming, G. R.; Beddard, G. S.; Robinson, G. W.; Thistlethwaite, P. J.; Woolfe, G. J. Photophysics of Aqueous Tryptophan - Ph and Temperature Effects. Journal of the American Chemical Society 1980, 102 (20), 6271-6279.

93. Sobolewski, A. L.; Domcke, W. Photoinduced charge separation in indole-water clusters. Chemical Physics Letters 2000, 329 (1-2), 130-137.

94. Tolbert, L. M.; Harvey, L. C.; Lum, R. C. Excited-State Proton-Transfer from Hydroxyalkylnaphthols. Journal of Physical Chemistry 1993, 97 (50), 13335-13340.

95. Bent, D. V.; Hayon, E. Excited-State Chemistry of Aromatic Amino-Acids and Related Peptides .3. Tryptophan. Journal of the American Chemical Society 1975, 97 (10), 2612-2619.

96. Eftink, M. R.; Jia, Y. W.; Hu, D.; Ghiron, C. A. Fluorescence Studies with Tryptophan Analogs - Excited-State Interactions Involving the Side-Chain Amino Group. Journal of Physical Chemistry 1995, 99 (15), 5713-5723.

97. Urabe, K.; Aroca, P.; Tsukamoto, K.; Mascagna, D.; Palumbo, A.; Prota, G.; Hearing, V. J. The Inherent Cytotoxicity of Melanin Precursors - A Revision. Biochimica et Biophysica Acta-Molecular Cell Research 1994, 1221 (3), 272-278.

98. Rele, M.; Kapoor, S.; Hegde, S.; Naumov, S.; Mukherjee, T. Photophysical characteristics and density functional theory calculations of indole 2-carboxylic acid in the presence of mercurous ions. Research on Chemical Intermediates 2006, 32 (7), 637-645.

99. Hattig, C.; Hald, K. Implementation of RI-CC2 triplet excitation energies with an application to trans-azobenzene. Physical Chemistry Chemical Physics 2002, 4 (11), 2111-2118.

100. Charkoudian, L. K.; Franz, K. J. INOR 614-Development of iron chelators triggered by reactive oxygen species. Abstracts of Papers of the American Chemical Society 2006, 232.

101. Olsen, S.; Riesz, J.; Mahadevan, I.; Coutts, A.; Bothma, J. P.; Powell, B. J.; McKenzie, R. H.; Smith, S. C.; Meredith, P. Convergent proton-transfer photocycles violate mirror-image symmetry in a key melanin monomer. Journal of the American Chemical Society 2007, 129 (21), 6672-6673.

102. Gauden, M.; Pezzella, A.; Panzella, L.; Neves-Petersen, M. T.; Skovsen, E.; Petersen, S. B.; Mullen, K. M.; Napolitano, A.; d'Ischia, M.; Sundstrom, V. Role of Solvent, pH, and Molecular Size in Excited-State Deactivation of Key Eumelanin Building Blocks: Implications for Melanin Pigment Photostability. Journal of the American Chemical Society 2008, 130 (50), 17038-17043.

103. Huijser, A.; Pezzella, A.; Hannestad, J. K.; Panzella, L.; Napolitano, A.; d'Ischia, M.; Sundstrom, V. UV-Dissipation Mechanisms in the Eumelanin Building Block DHICA. Chemphyschem 2010, 11 (11), 2424-2431.

104. Rosenthal, S. J.; Jimenez, R.; Fleming, G. R.; Kumar, P. V.; Maroncelli, M. Solvation Dynamics in Methanol - Experimental and Molecular-Dynamics Simulation Studies. Journal of Molecular Liquids 1994, 60 (1-3), 25-56.

105. Jimenez, R.; Fleming, G. R.; Kumar, P. V.; Maroncelli, M. Femtosecond Solvation Dynamics of Water. Nature 1994, 369 (6480), 471-473.

106. Tolbert, L. M.; Harvey, L. C.; Lum, R. C. Excited-State Proton-Transfer from Hydroxyalkylnaphthols. Journal of Physical Chemistry 1993, 97 (50), 13335-13340.

107. Gauden, M.; Pezzella, A.; Panzella, L.; Napolitano, A.; d'Ischia, M.; Sundstrom, V. Ultrafast Excited State Dynamics of 5,6-Dihydroxyindole, A Key Eumelanin

Building Block: Nonradiative Decay Mechanism. Journal of Physical Chemistry B 2009, 113 (37), 12575-12580.

108. Sobolewski, A. L.; Domcke, W. Photophysics of eumelanin: Ab initio studies on the electronic spectroscopy and photochemistry of 5,6-dihydroxyindole. Chemphyschem 2007, 8 (5), 756-762.

109. Ohman, H.; Vahlquist, A. In-Vivo Studies Concerning A Ph Gradient in Human Stratum-Corneum and Upper Epidermis. Acta Dermato-Venereologica 1994, 74 (5), 375-379.

110. Pezzella, A.; Iadonisi, A.; Valerio, S.; Panzella, L.; Napolitano, A.; Adinolfi, M.; d'Ischia, M. Disentangling Eumelanin "Black Chromophore": Visible Absorption Changes As Signatures of Oxidation State- and Aggregation-Dependent Dynamic Interactions in a Model Water-Soluble 5,6-Dihydroxyindole Polymer. Journal of the American Chemical Society 2009, 131 (42), 15270-15275.

111. Manca, C.; Tanner, C.; Leutwyler, S. Excited state hydrogen atom transfer in ammonia-wire and water-wire clusters. International Reviews in Physical Chemistry 2005, 24 (3-4), 457-488.

112. Tanner, C.; Manca, C.; Leutwyler, S. 7-hydroxyquinoline center dot(NH3)(3): A model for excited state H-atom transfer along an ammonia wire. Chimia 2004, 58 (4), 234-236.